Reliability Engineering and System Safety 277 (2027) 113356

Contents lists available at ScienceDirect

Reliability Engineering and System Safety

journal homepage: www.elsevier.com/locate/ress

# Hierarchical relationships analysis: A novel data-driven framework to assess the influential factors of marine accidents

Yinwei Feng [a,b,c], Xinjian Wang [a,b,*], Yuhao Cao [b,*], Jingen Zhou [d], Jin Wang [b], Zaili Yang [b,e]

[a] Navigation College, Dalian Maritime University, Dalian, 116026, PR China
[b] Liverpool Logistics, Offshore and Marine (LOOM) Research Institute, Liverpool John Moores University, Liverpool, L3 3AF, UK
[c] Department of Logistics and Maritime Studies, The Hong Kong Polytechnic University, Hong Kong, 999077, PR China
[d] Department of Operations Management, Supply Chain and Information Systems, KEDGE business school, Marseille, 13288, France
[e] School of Civil and Environment Engineering, Nanyang Technological University, 50 Nanyang Avenue, 639798, Singapore

ARTICLE INFO

*Keywords:*
Maritime safety
Maritime accident
Data-driven framework
Machine learning
Association rule mining
DEMATEL

ABSTRACT

Marine accidents are associated with multiple risk influential factors (RIFs), whose interrelationships complicate risk analysis. Existing approaches rarely connect associations among factor states with data-driven influence analysis and weighted hierarchical interpretation. To address above gaps, this study proposes a combined hierarchical analysis framework integrating Combined Association Rule Mining (CARM), data-driven Decision-Making Trial and Evaluation Laboratory (DEMATEL), and a maximum mean de-entropy-based Weighted Total Adversarial Interpretive Structural Model (MMDE-WTAISM). CARM aggregates associations among RIF states into directed factor-level relationships using an expectation-based combined-conviction metric. DEMATEL quantifies direct and indirect network influence with a data-driven transform method. MMDE-WTAISM selects an adaptive threshold and incorporates DEMATEL relationship strengths into weighted indicators and complementary UP-type and DOWN-type hierarchies. The analysis generated 826 factor-level rules, retained 120 direct relationships, and identified 258 reachable relationships, two feedback clusters, and four computational levels. In the full sample, ship certificates, seafarer certificates, manning, regulation, and education and training had the five highest weighted driving-power values. A 1,000-replicate bootstrap of the complete analytical pipeline supported the sampling stability of the principal results. The framework provides a reproducible route from associations among factor states to weighted bidirectional hierarchies without expert scoring, supporting targeted maritime safety governance and operational risk control.

## 1. Introduction

Commercial shipping carries roughly four-fifths of world merchandise trade by volume, so its reliability is inseparable from the functioning of international supply chains [1,57]. With such a large volume, ensuring the safe and smooth operation of ships guarantees the benefits of the market [2]. However, according to the reports published by global maritime authorities, marine accidents continue to occur every year [3]. The Transportation Safety Board of Canada (TSB) received 990 reports of marine transportation occurrences in 2025, including 257 accidents, 733 incidents, 6 fatalities, and 45 serious injuries (Transportation Safety Board of [4]). Within the European Maritime Casualty Information Platform scope, 2,659 casualties and incidents involving 2,864 ships were reported for 2024; the 2015-2024 total was 26,751, or approximately 2,675 per year (European Maritime Safety [5]). The United Kingdom's Marine Accident Investigation Branch separately received 1, 263 accident reports in 2022 (Marine Accident Investigation [6]). Behind these numbers, evidence has proven that marine accidents pose a threat to the lives of people and the safety of property [7]. A number of notable marine accidents have resulted in substantial losses to human safety and economic markets [8,9]. For instance, on 16 April 2014, there was a world-shocking sinking accident in the Republic of Korea. The sinking of a passenger ship named “Sewol” resulted in the deaths of 304 people, due to overloading, improper loading and crew negligence [10]. During the investigation of these shocking cases, these serious marine accidents have revealed that complex factors contribute to marine

* Corresponding authors.
*E-mail addresses:* wangxinjian@dlmu.edu.cn (X. Wang), Y.Cao@ljmu.ac.uk (Y. Cao).

https://doi.org/10.1016/j.ress.2026.113356
Received 11 January 2025; Received in revised form 18 August 2026; Accepted 21 August 2026
Available online 22 August 2026

accidents [11]. Naturally, this raises a question for stakeholders: if the influential factors and their interconnections can be identified and studied, could this provide insights and strategies to alleviate accident severity so that the evolution and even the occurrence of accidents can be controlled? Therefore, as a significant research topic in maritime safety, marine accident relevant studies have never been lacking. Accordingly, marine-accident research has advanced from both factor-oriented and methodological perspectives, including the investigation of Risk Influential Factors (RIFs) and the development of analytical approaches for accident risk assessment [12].

Prior studies commonly organise marine-accident information into human, ship, environmental, management, and accident-context categories [11]. During this period, relying on well-established databases, researchers have employed diverse methodologies to delve into how these RIFs influence marine accidents. Table 1 reviews the literatures related to the marine accident exploration methods, including the application, strength and weakness. From Table 1, it can be known that current research includes qualitative assessments (e.g., HFACS), quantitative analysis (e.g., BN), decision support (e.g., tree-based analysis), categorisation discussions (e.g., clustering analysis), etc. These methods offer complementary capabilities: some organise accident evidence and identify contributing factors, whereas others quantify probabilistic dependencies or reveal structural relationships within a risk system. However, the approaches reviewed above do not simultaneously support scalable pattern discovery, factor-level influence analysis, and hierarchical interpretation. The resulting methodological gap therefore concerns the integration of these analytical capabilities rather than the absence of methods for marine-accident analysis.

Based on Table 1, the Association Rule Mining (ARM) emerges as a commonly used mining technique and exhibits its advantages in discovering implicit interrelationships within extensive datasets. This functional benefit allows ARM to run quickly on large datasets to provide preliminary insights without the need for preconceived hypothesis [13]. However, although ARM can quantify associative relationships among RIFs through parameters such as support, lift, and confidence, it provides limited theoretical support for causal-influence interpretation or in-depth quantitative analysis of marine accidents. In this regard, other methods like BN seem to present an appealing alternative for a holistic visualization of accident risks. Yet, constructing an accurate BN model requires in-depth domain knowledge and a series of predefined probabilistic distributions, making the process potentially time-intensive and susceptible to subjective biases [14], sometimes even impossible when the data is presented at a small scale compared to the size of the networks. Moreover, while BN can map out probabilistic dependencies among factors, these connections do not necessarily imply natural causality in practice but more sensible statistically, thus providing limited, or even sometimes misleading insights into the causative mechanisms of marine accidents. Recent reliability-oriented studies have further advanced data-driven maritime-risk analysis by combining historical collision reports with Apriori-based association analysis, entropy weighting, and BP-DEMATEL [15], and by integrating HFACS with Bayesian networks to identify human and organisational factors and accident-development paths [16]. Scenario-oriented Bayesian-network models have also improved collision-risk deduction and maritime-safety assessment, but the reviewed approaches do not simultaneously integrate factor-level association aggregation, adaptive screening of the DEMATEL influence network, preservation of heterogeneous relationship strengths, and bidirectional hierarchical extraction [17,18]. Therefore, the above review reveals a significant methodological gap in marine accident RIF research: the need for a data-driven framework that can objectively mine large-scale accident data while supporting causal-influence analysis and hierarchical structural interpretation.

DEMATEL and ISM have been paired in applications ranging from logistics and offshore engineering to marine ranching, urban gas pipelines, and inland-waterway transport [19–21]. In such combinations, a continuous influence network is quantified first and then translated into hierarchical positions. These positions describe structural placement in the network; they should not be read as a universal temporal sequence of accident events.

Existing DEMATEL-ISM applications illustrate the combined use of influence quantification and hierarchical decomposition in contexts

**Table 1**
Comparative analysis of methods of marine accident studies.

| Method | Literature | Application | Strength | Weakness |
|---|---|---|---|---|
| Human Factors Analysis and Classification System (HFACS) | [24,25] | A framework to identify the human error from 4 categories. | •Strong adaptability<br>•Short training time<br>•Wide acceptance | •Oversimplification<br>•Lack of detail |
| Formal safety assessment (FSA) | [26] | A systematic approach to assess and manage the navigational risks. | •Comprehensiveness assessment<br>•Risk quantification | •Data and time requirements<br>•Complexity and subjectivity |
| Tree-based analysis methods | [27,28] | A systematic to identify the causes and to determine the starting point of the event chain. | •Systematic assessment<br>•Fault Tree Analysis can help identify root causes. | •Data and time requirements<br>•Event chain complexity |
| Fuzzy theory | [29,30] | A fuzzy modelling method to address the uncertainty and ambiguity, typically combining with other methods. | •Uncertainty handling<br>•Multi-factor integration<br>•Flexibility | •Subjectivity<br>•Higher data requirements<br>•Computational complexity |
| Regression models | [31] | A data-driven method to assess the historical accident data and the relevant factors, so as to test and predict the occurrence trend. | •Data-driven<br>•Explain ability<br>•Trend analysis | •Higher data requirements<br>•Difficulty in considering complex interactions between factors |
| Association rule mining (ARM) | [32] | A mining technique to explore the associations among data and identify the critical variables. | •Data-driven<br>•Simplicity and straightforwardness<br>•Discovering unknown relationships | •Non-causal relationship<br>•Parameter threshold setting<br>•Neglect of other factors |
| Analytic hierarchy process (AHP) | [30] | A multi-criteria decision-making approach to assess the weights and impact of different risks and rank the factors. | •Multi-criteria decision making<br>•Structural analysis<br>•Quantifiable results<br>•Consistency checking | •Subjectivity in judgement matrices and weight allocation<br>•Expertise and data required |
| Bayesian network (BN) | [14,33] | A directed acyclic graph capable of probabilistically modelling the correlations and probability distributions between risk nodes. | •Data-driven<br>•Probability modelling<br>•Causality modelling | •Modelling accuracy<br>•Higher data requirements<br>•Subjectivity in modelling |
| Complex network (CN) | [34,35] | A network modelling approach to establish relationships between factors and simulate the path of risk propagation. | •Comprehensiveness<br>•Visualisation<br>•Key node identification | •Higher data requirements<br>•Computational complexity |

such as urban gas-pipeline accidents, marine-ranching risk, and mine-water inrush [22]. This further demonstrates the versatility of this integrated approach. Typically, from the existing applications, expert opinion or questionnaires are the primary data sources to calculate the matrix weights and then fed into the overall framework via DEMATEL. Although data based on expert knowledge or typical cases can reflect a realistic and cognitively correct situation, this also tends to be influenced by subjectivity [23]. Therefore, to exploit the causal-influence analysis and structural-modelling capabilities of this combined approach while improving objectivity, a reliable data-driven methodology is needed to strengthen the integrated framework and advance accident analysis in general and marine accident assessment in particular.

Within this methodological framework, ISM converts inter-factor relationships into a binary reachability structure and then decomposes the resulting network into hierarchical levels. Conventional ISM generally produces a single hierarchy from a binary relationship matrix. TAISM extends this logic by applying complementary result-priority and cause-priority extraction rules, thereby generating UP-type and DOWN-type hierarchies and providing two perspectives for interpreting systems containing feedback, mutual dependence, and strongly connected relationships. Recent applications in artificial-intelligence talent development, adolescent behavioural-risk analysis, and construction-enterprise digital transformation have demonstrated the usefulness of DEMATEL-TAISM for examining complex systems from these complementary hierarchical perspectives [36,37]. However, the hierarchical structure obtained by TAISM is sensitive to how the continuous DEMATEL total-relation matrix is converted into a binary representation. Cut-offs determined by sample averages or expert judgement may remove relationships that still carry useful structural information [38]. MMDE provides a data-responsive alternative by determining the cut-off from the dispatching and receiving information contained in DEMATEL relationships, and was originally introduced for threshold determination in DEMATEL analysis [39]. Its applications to mining safety, renewable-fuel development, and sustainable-agriculture technology adoption further support its use as a reproducible screening procedure prior to hierarchical modelling [38,40,41]. A related stream of weighted structural modelling also suggests that retaining quantitative differences among relationships can improve the discrimination of factor importance and driving–dependence characteristics beyond a purely binary representation [42]. Building on these two complementary streams, the MMDE-WTAISM developed in this study separates relationship screening from relationship-strength interpretation. MMDE determines which DEMATEL relationships are retained, whereas the corresponding DEMATEL values provide the relationship strengths used in the weighted analysis. Binary reachability is used for strongly connected component identification and bidirectional hierarchical extraction, while the weighted relationship matrix supports the calculation of weighted driving, dependence, net-driving, and comprehensive-importance indicators.

The preceding review points to three unresolved methodological issues in the analysis of marine-accident RIFs. These issues also define the methodological contributions made in this study.

(1) Conventional ARM operates primarily on associations between particular factor states, leaving the resulting evidence disconnected from directed factor-level influence analysis. CARM is therefore introduced to consolidate state-level association evidence through an expectation-based combined conviction metric, yielding directed relationships between factors that can be passed to DEMATEL.
(2) The hierarchical outcome of TAISM is conditioned by the rule used to retain relationships, and subsequent binarisation removes differences in the magnitudes of the retained DEMATEL influences. The proposed MMDE-WTAISM addresses these two issues by using an MMDE-derived cut-off for relationship selection while preserving the associated DEMATEL values for weighted structural evaluation and complementary UP-type and DOWN-type hierarchical extraction.
(3) More broadly, the analytical functions represented by association mining, influence quantification, relationship screening, and bidirectional hierarchical interpretation remain fragmented across the reviewed literature. This study connects these functions through CARM, data-driven DEMATEL, and MMDE-WTAISM in a unified reproducible framework, with the factor-level relationships obtained from accident data replacing the conventional reliance on an expert-scored direct-influence matrix.

Taken together, these methodological components allow the RIF system to be examined in terms of association structure, weighted influence, feedback relationships, and hierarchical location. Their joint interpretation further differentiates long-term governance priorities, intermediate transmission factors, and operationally observable risk conditions, providing evidence for maritime policy and safety-management decisions.

The remainder of the paper follows the methodological and analytical sequence of the study. Section 2 presents the dataset and the CARM, DEMATEL, and MMDE-WTAISM methods, while Section 3 reports the corresponding analytical results and evaluates their sampling stability. Section 4 interprets these findings from theoretical and practical perspectives, followed by the conclusions in Section 5.

## 2. Methodology

Fig. 1 summarises the analytical sequence. The 1,294-record dataset first supplies state-level evidence to CARM; the resulting factor-level relationships form the direct input to data-driven DEMATEL; and MMDE-WTAISM screens, weights, and hierarchically interprets the downstream influence structure. Sections 2.1-2.4 specify each module.

### *2.1. Dataset*

The analysis reuses the consolidated accident database documented in the authors' earlier work [11]. Reports issued by different authorities for the same event were linked and represented by a single record, yielding 1,294 consolidated investigations covering 2000-2019. The model retains 31 RIFs organized into five domains: human, vessel, management, environment, and accident information. Their codes, recorded states, and operational definitions are provided in Table A1, Appendix A.

### *2.2. Combined association rule mining (CARM)*

The ARM is a pivotal data mining technique capable of discovering meaningful co-occurrences and associations within the complex and ambiguous chaotic data [43,58]. When applying ARM, support, confidence and lift degrees are the key parameters to express the interrelationships. In the study of marine accidents, the accident records are typically saved in a csv file. For the ARM analysis, each consolidated accident record was encoded as a vector of observed RIF states. Therefore, the quantitative values derived from this data reflect the relationships between the states of these RIFs [32,44]. For example, using the explicit form to express the effect: $Support(A_i)$ indicates the frequency of the occurrence of the *i-th* state of RIF *A*; $Confidence(A_i \Rightarrow B_j)$ indicates the probability of the occurrence of the *j-th* state of RIF *B* (i.e., consequent) in the presence of the *i-th* state of RIF *A* (i.e., antecedent). $Lift(A_i \Rightarrow B_i)$ indicates the enhancement effect of the *i-th* state of RIF *A*'s appearance on the probability of the *j-th* state of RIF *B*'s appearance. If $Lift(A_i \Rightarrow B_i) \geq 1$, it indicates a facilitating effect. Therefore, the attribute of lift is commonly used to screen effective association rules. However, as previously highlighted, the traditional ARM technique can only

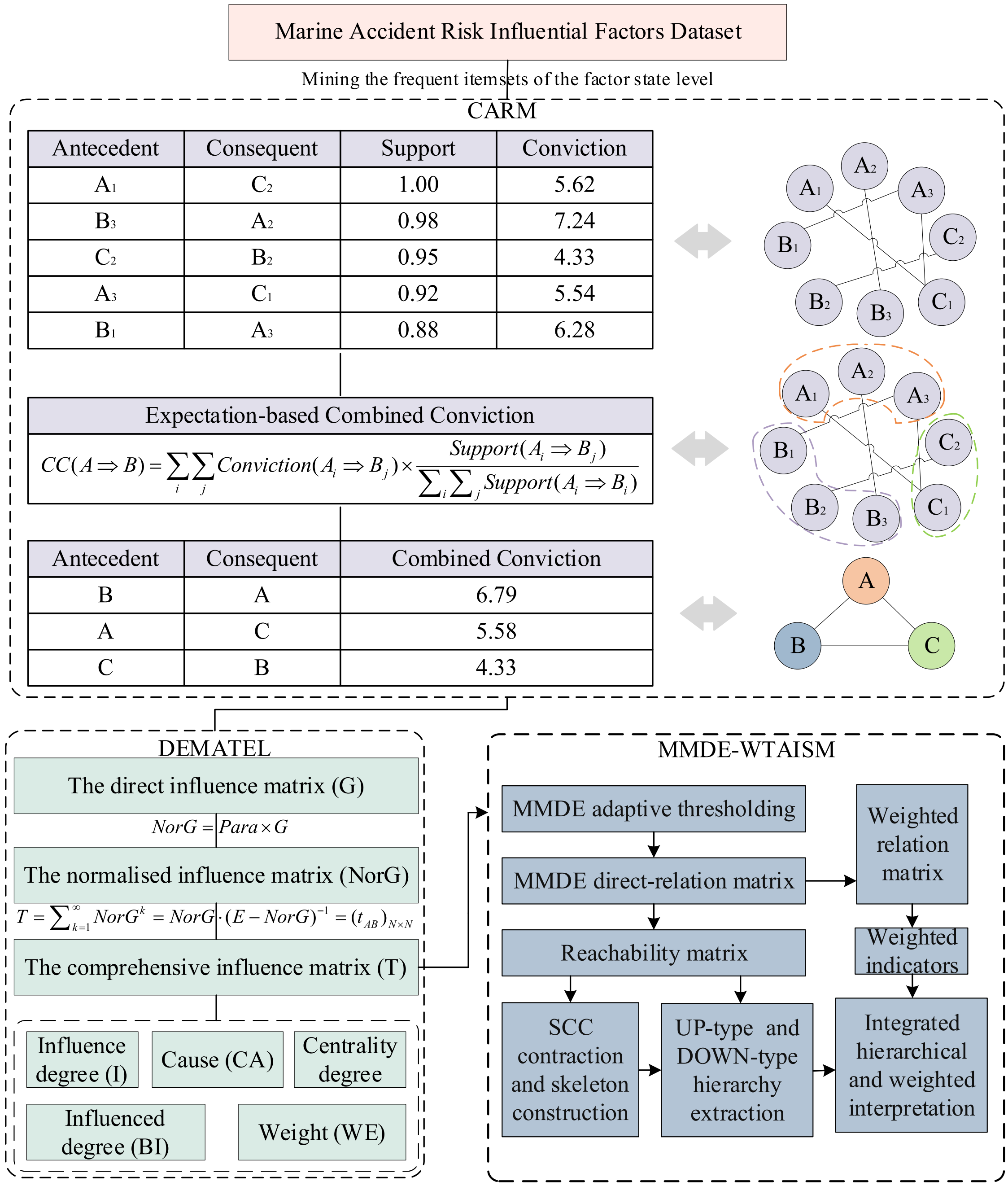


**Fig. 1.** The proposed data-driven framework for RIFs analysis of marine accidents. (Note: For explanations of the formulas and symbols used in this figure, please refer to Sections 2.2 to 2.4.).

obtain the results in a lower state level and cannot obtain the association relationship in the higher factor level.

Accordingly, CARM extends the conventional ARM procedure by aggregating association evidence across RIF states into directed factor-level relationships. This aggregation is performed using the expectation-based combined conviction (CC), which forms a support-weighted expectation of state-level conviction values to characterize the directional association between an antecedent factor and a consequent factor, as defined in Eq. (1).

$$CC(A\Rightarrow B) = \sum_i \sum_j Conviction(A_i\Rightarrow B_j) \times \frac{Support(A_i\Rightarrow B_j)}{\sum_i \sum_j Support(A_i\Rightarrow B_i)} \tag{1}$$

where $Conviction(A_i\Rightarrow B_j) = (1 - Support(B_j))/(1 - Confidence(A_i\Rightarrow B_j))$; $Support(A_i\Rightarrow B_j)$ indicates the probability of the occurrence of association rule of $A_i\Rightarrow B_j$. Specifically, the conviction measures the ratio between the expected probability of $A_i$ occurring and $B_j$ not occurring under the assumption that $A_i$ and $B_j$ are independent (i.e. the association rule is invalid) and the actual frequency of $A_i$ occurring and $B_j$ not occurring observed in the data. In that case, the conviction measures the dependence degree of the consequent on the antecedent within an association rule, where the larger conviction, the higher dependence. An important property of conviction is the asymmetry with respect to the support of the itemset. This means that for the rule of "$A_i\Rightarrow B_j$" and the rule of "$B_j\Rightarrow A_j$", even if they have the same support and confidence, their conviction may be different, which helps to reveal more information in rule evaluation.

In Eq. (1), $A$ and $B$ are different RIFs, $A_i$ and $B_j$ are different states, where $A_i \in A$ and $B_i \in B$. Through support-weighted aggregation of the retained state-pair convictions, CC produces one directional association value for each RIF pair, improving factor-level interpretability. Particularly, by combining all possible state pairs, CC may be less sensitive to the effect of a single or a few anomalous state pairs, and thus may provide a more robust association measure. Additionally, by setting a support threshold, association rules in state-level that are very low probability are filtered out. This approach not only mitigates the problem of significant changes in factor-lever rules caused by the dominance of low-probability events but also reduces the resource burden in real-time processes where addressing such events might yield insufficient returns. This will provide a reliable theoretical basis and data support for the next step of integration with DEMATEL.

### 2.3. Decision-making trial and evaluation laboratory

Marine accidents are complex events influenced by a series of interdependent and interacting factors [11]. Compared with other methods (e.g., CNs and system dynamics), DEMATEL has the advantage of being able to deal with and analyse the dynamic interactions between factors, explicitly revealing the direct and indirect causality between factors in a marine accident [8,19]. By analysing the topological metrics of RIFs, DEMATEL can help to identify critical factors in marine accidents and present the quantitative insights of the relationships between factors. In addition, the flexibility of DEMATEL allows it to be adapted and customized. In the practice of coupling with some methods, e.g. with ISM [22,45], Fuzzy Cognitive Map [46] and Analytic Network Process [47], etc., DEMATEL often serves as a front-loading tool for key factor identification and interaction relationship revealing, demonstrating its powerful parsing and coupling capabilities.

Traditionally, DEMATEL requires a team of experts to help determine the level of influence between factors to be used as input data. However, the validity of expert opinions and the setting of weights potentially introduce subjective interference and uncertainty. Therefore, to address it, this study adopts a new data-driven approach to construct DEMATEL model. Eq. (2) arranges the CARM derived factor-level values in the direct-influence matrix G.

$$G = \begin{array}{c c} & \begin{array}{cccc} Fa_1 & Fa_2 & \cdots & Fa_N \end{array} \\ \begin{array}{c} Fa_1 \\ Fa_2 \\ \vdots \\ Fa_N \end{array} & \begin{bmatrix} g_{11} & g_{12} & \cdots & g_{1N} \\ g_{21} & g_{22} & \cdots & g_{2N} \\ \vdots & \vdots & g_{AB} & \vdots \\ g_{N1} & g_{N2} & \cdots & g_{NN} \end{bmatrix} \end{array} \tag{2}$$

where $g_{AB} = e_{AB} \times CC(A \Rightarrow B)$. $g_{AB}$ denotes the influential degree of RIF $A$ on RIF $B$; $e_{AB}$ denotes the influence coefficient, $e_{AB} = 1$ indicates that there is an association from RIF $A$ to RIF $B$, while $e_{AB} = 0$ indicates there is no association. $N$ is the size of the RIF set, and $Fa_N$ is its final indexed element. Therefore, the results of the CARM are treated as the input of the DEMATEL model, achieving the organic coupling of the two methods.

Eqs. (3) and (4) scale G to obtain $NorG$.

$$NorG = Para \times G \tag{3}$$

$$Para = \left[\max(r_1, r_2, \ldots, r_N)^2 + \max(c_1, c_2, \ldots, c_N)^2\right]^{-1/2} \tag{4}$$

Here, $Para$ is the normalization parameter, while $r_i$ and $c_i$ denote the sums of row $i$ and column $i$ of $G$, respectively. Eq. (5) accumulates the direct and indirect effects represented by $NorG$ in the comprehensive influence matrix $T$.

$$T = \sum_{k=1}^{\infty} NorG^k = NorG \cdot (E - NorG)^{-1} = (t_{AB})_{N \times N} \tag{5}$$

where the comprehensive influence matrix $T$ contains $N$ rows and $N$ columns; $E$ denotes the identity matrix; '·' denotes the matrix inner product; $t_{AB}$ denotes the comprehensive influence element from RIF $A$ to RIF $B$ within the comprehensive influence matrix. Notably, Eq. (5) is valid under the conditions that all matrix entries lie within the closed unit interval [0,1] and that all diagonal entries vanish, i.e., the factors do not affect themselves [8,48].

The outgoing influence, incoming influence, centrality, net influence, and normalized weight of each RIF are then calculated from $T$ using Eqs. (6)–(10):

$$I_A = \sum_B t_{AB} \tag{6}$$

$$BI_A = \sum_B t_{BA} \tag{7}$$

$$CE_A = I_A + BI_A \tag{8}$$

$$CA_A = I_A - BI_A \tag{9}$$

$$WE_A = \frac{\left(CE_A^2 + CA_A^2\right)^{1/2}}{\sum_A \left(CE_A^2 + CA_A^2\right)^{1/2}} \tag{10}$$

For RIF $A$, $I_A$ and $BI_A$ sum its outgoing and incoming influence, respectively. $CE_A$ is their sum, $CA_A$ is their difference, and $WE_A$ is the normalized magnitude defined in Eq. (10).

### 2.4. MMDE-based weighted total adversarial interpretive structural model (MMDE-WTAISM)

The ISM is an approach to analysing and structuring the interaction between elements in complex problems [49]. It is a structured methodology that graphically represents the hierarchy between individuals or factors by identifying and aggregating their interrelationships. In an integrated workflow, DEMATEL propagates the initial relations to quantify network-wide influence, ISM then organizes the resulting dependency pattern into hierarchical levels [22,45,21]. However, the original ISM framework typically extracts a single hierarchy from a binary relationship matrix. TAISM extends this logic by introducing adversarial UP-type and DOWN-type extraction procedures, which provide two complementary perspectives for hierarchical interpretation. Nevertheless, the original TAISM relationship-construction process still has two limitations. First, the empirical thresholding rule may not adapt sufficiently to the structural distribution of the DEMATEL comprehensive influence matrix. Second, binary relationship screening indicates whether a relationship is retained but discards the influence-intensity information contained in the DEMATEL matrix.

To address these limitations, this section introduces the MMDE-based Weighted Total Adversarial Interpretive Structural Model (MMDE-WTAISM), which serves as the downstream hierarchical interpretation module of the proposed framework. The method retains the adversarial UP-type and DOWN-type extraction logic of TAISM, but replaces the original empirical thresholding strategy with an MMDE-derived adaptive threshold and incorporates weighted indicators derived from the DEMATEL comprehensive influence matrix. Therefore, the revised module can describe not only whether one RIF can reach another, but also how strongly the retained relationships contribute to driving and comprehensive importance.

Using $T$ from Section 2.3, MMDE-WTAISM performs adaptive screening, preserves the retained influence strengths, and extracts UP-type and DOWN-type hierarchies through the stages below.

(1) Derive the MMDE-screened relationship matrix.

The off-diagonal entries of $T$ in Eq. (11) are treated as candidate directed influences; $t_{AB}$ denotes the influence of RIF A on RIF B, and $N$ is the number of RIFs. After the diagonal entries are excluded, these values form the candidate set $\Omega$ in Eq. (12). All candidate influence values in $\Omega$ are then sorted in descending order according to influence intensity, generating the ordered sequence in Eq. (13). In Eq. (13), $L = N(N-1)$ denotes the total number of off-diagonal candidate directed relationships. The MMDE-derived threshold is selected through a sequential candidate-evaluation process. Specifically, each candidate position $k$ along the ordered influence sequence is examined. For a given $k$, the leading $k$ relationships constitute the candidate prefix, while the remaining relationships form its complement, as defined in Eq. (14).

$$T = (t_{AB})_{N\times N} \tag{11}$$

$$\Omega = \{t_{AB} | A \neq B,\ A, B = 1, 2, \dots, N\} \tag{12}$$

$$t_{(1)} \geq t_{(2)} \geq \dots \geq t_{(L)}, \quad L = N(N-1) \tag{13}$$

$$\Omega_k^+ = \{t_{(1)}, \dots, t_{(k)}\}, \quad \Omega_k^- = \{t_{(k+1)}, \dots, t_{(L)}\}, \quad k = 1, 2, \dots, L-1 \tag{14}$$

For each candidate position $k$, the corresponding mean-de-entropy score, denoted asMMDE($k$), is calculated from the dispatching and receiving distributions of the relationships in the leading candidate prefix. The MMDE-optimal candidate boundary position $k^*$ is determined by maximizing MMDE($k$), as shown in Eq. (15). The adaptive threshold is then set equal to the influence value at this boundary, $\lambda_{MMDE} = t_{(k^*)}$, as shown in Eq. (16). Because the direct relationship matrix applies the strict retention rule $t_{AB} > \lambda_{\mathrm{MMDE}}$, the relationship at the boundary is not retained. Accordingly, $k^*$ denotes the MMDE-optimal candidate boundary position rather than the number of retained relationships. Based on the adaptive threshold in Eq. (16), the MMDE-based direct relationship matrix $R^{MMDE}$ is constructed, as shown in Eq. (17). Each element $r_{AB}^{\mathrm{MMDE}}$ is then determined according to the binary retained relationship rule in Eq. (18).

$$k^* = \mathrm{argmax}_{1 \leq k < L} \mathrm{MMDE}(k) \tag{15}$$

$$\lambda_{MMDE} = t_{(k^*)} \tag{16}$$

$$R^{MMDE} = (r_{AB}^{MMDE})_{N\times N} \tag{17}$$

$$r_{AB}^{MMDE} = \begin{cases} 1, & t_{AB} > \lambda_{MMDE} \text{ and } A \neq B, \\ 0, & \text{otherwise.} \end{cases} \tag{18}$$

In this step, $R^{MMDE}$ represents the direct relationships retained by the MMDE-derived adaptive threshold. Compared with the original empirical thresholding rule, this process screens the retained relationship structure from the distribution of DEMATEL influence values rather than relying only on a fixed mean-plus-standard-deviation cut-off.

(2) Compute the reachability matrix $M$ through Boolean iteration [49].

Based on the MMDE-based direct relationship matrix $R^{MMDE}$, the reachability matrix $M$ is obtained through Boolean operations as in ISM/TAISM. The identity matrix $E$ is first added to $R^{MMDE}$ to include self-reachability. The Boolean product operation is then iteratively performed according to Eq. (19) until the transition matrix reaches a stable state. The resulting reachability matrix $M$ is defined in Eq. (20).

$$B_1 = R^{MMDE} + E, \quad B_2 = B_1 \odot B_1, \quad B_3 = B_2 \odot B_1, \dots, \quad B_n = B_{n-1} \odot B_1 \tag{19}$$

$$M = (m_{AB})_{N\times N} = B_n, \quad B_n = B_{n-1} \tag{20}$$

Here, $B_n$ is the transition matrix obtained after $n$ Boolean updates, and the operator in Eq. (19) denotes Boolean matrix multiplication. Once $B_n = B_{(n-1)}$, the iteration has converged and the fixed point defines $M$.

(3) Construct the weighted relationship matrix.

Although $R^{MMDE}$ and $M$ are necessary for binary reachability analysis, a purely binary relationship matrix cannot express the strength of the retained influence relationships. To avoid losing the influence-intensity information contained in DEMATEL, MMDE-WTAISM further constructs a weighted relationship matrix $W^{MMDE}$, as defined in Eq. (21). Each retained binary relationship is assigned its corresponding comprehensive influence value from $T$ according to Eq. (22).

$$W^{MMDE} = (w_{AB}^{MMDE})_{N\times N} \tag{21}$$

$$w_{AB}^{MMDE} = r_{AB}^{MMDE} \times t_{AB} \tag{22}$$

This weighted design does not modify the upstream CARM and DEMATEL results. Instead, it preserves DEMATEL-derived influence intensity on the retained MMDE-WTAISM relationships and provides the quantitative basis for the subsequent weighted indicators.

(4) Calculate weighted indicators.

Four weighted indicators are calculated from $W^{MMDE}$ to support the interpretation of retained influence intensity. Weighted driving power (WDP) measures the total retained outgoing weighted influence of a RIF, as shown in Eq. (23). Weighted dependence power (WDE) measures the total retained incoming weighted influence, as shown in Eq. (24). Weighted net driving (WND) describes the balance between outgoing and incoming weighted influence, as shown in Eq. (25). Weighted comprehensive importance (WCI) measures the overall weighted involvement of each RIF in the retained relationship structure, as shown in Eq. (26).

$$WDP_A = \sum_{B=1}^{N} w_{AB}^{MMDE} \tag{23}$$

$$WDE_A = \sum_{B=1}^{N} w_{BA}^{MMDE} \tag{24}$$

$$WND_A = WDP_A - WDE_A \tag{25}$$

$$WCI_A = WDP_A + WDE_A \tag{26}$$

These indicators complement the binary reachability hierarchy by identifying factors that are not only structurally reachable but also influential in terms of DEMATEL-derived intensity.

(5) Extract hierarchical levels in both directions.

Level assignment in the UP-type and DOWN-type hierarchies is governed by the reachability set, prior sets, and the intersection of reachable and prior sets. The formulations are shown in Eqs. (27), (28) and (29).

$$RS(Fa_A) = \{Fa_B | m_{AB} = 1\} \tag{27}$$

$$QS(Fa_A) = \{Fa_B | m_{BA} = 1\} \tag{28}$$

$$TS(Fa_A) = RS(Fa_A) \cap QS(Fa_A) \tag{29}$$

where $RS(Fa_A)$ denotes the reachable set of $Fa_A$, i.e., the set of the RIFs that have the elements equal to 1 in the $A$-*th* row of the reachable matrix. $QS(Fa_A)$ denotes the prior set of $Fa_A$, i.e., the set of RIFs whose corresponding elements equal 1 in the $A$-th column of the reachability matrix. $TS(Fa_A)$ denotes the intersection of reachable and prior sets.

During UP-type extraction, RIFs satisfying $RS(Fa_A) = TS(Fa_A)$ are assigned to the current top level; the selected RIFs are removed before the sets are recomputed. DOWN-type extraction assigns RIFs satisfying $QS(Fa_A) = TS(Fa_A)$ to the current bottom level, followed by the same removal-and-update cycle. Iteration ends after all RIFs have been assigned. Table B1 of Appendix B records the successive extractions.

(6) Identify strongly connected components and construct the skeleton relationship structure.

Construct the skeleton matrix $S$. In this step, Tarjan's algorithm is applied to solve for the strongly connected components of the reachable matrix [50]. In graph theory, a strongly connected component is a subgraph of a directed graph in which every pair of vertices is reachable from each other [51]. Therefore, the reduction matrix $ShM$ is constructed in this study to identify and merge each strongly connected component into a single node, as shown in Eq. (30). Based on the reduction matrix, the skeleton matrix is further derived to determine the links between the RIFs within the hierarchical structures, as shown in Eq. (31).

$$M \xrightarrow{\text{Tarjan}} ShM \tag{30}$$

$$S = ShM - (ShM - E) \odot (ShM - E) - E \tag{31}$$

(7) Interpret computational levels through functional strata.

The UP-type and DOWN-type extraction procedures assign RIFs to computational hierarchical levels through iterative set operations. For risk-management interpretation, these computational levels can be further organized into three functional strata: the uppermost computational level is interpreted as the surface stratum, the lowermost computational level is interpreted as the substantive stratum, and the intermediate computational levels are grouped into the transitional stratum. Thus, the functional strata are interpretive categories built on the computational hierarchy rather than additional algorithmic levels directly produced by the model.

## 3. Results

This section consists of three main parts. First, Section 3.1 applies the developed CARM algorithm to mine combined association rules from the marine accident dataset. Next, in Section 3.2, the combined association rule data is input into DEMATEL to identify the causal and effect RIFs within the marine accident system. Finally, Section 3.3 applies MMDE-WTAISM to the DEMATEL comprehensive influence matrix to obtain the adaptively screened, weighted, and bidirectional hierarchical structures of the RIF system.

### 3.1. CARM analysis

Based on the established dataset stated in Section 2.1, the CARM algorithm is applied to explore the association relationships among RIFs. Distinguished with traditional ARM, this study examines the associations at the factor level, rather than those between states. It is crucial to acknowledge that the outcomes derived from the CARM significantly depend on the configuration of its parameters. Setting appropriate threshold for support is essential to ensure that a balance is achieved between identifying significant associations and filtering out irrelevant noise. With the threshold of lift degree greater than 1, following multiple iterations and drawing insights from related research [52], the threshold for minimum support degree is determined as 0.005. Therefore, the prominent characteristics and the common links between the factors can be efficiently identified and extracted. Furthermore, the maximum limit for the restriction length is established at two, which guarantees that every node signifies a single RIF [59].

The CARM are programmed in Python, then 826 Combined Association Rules (CARs) are mined. The Top 10 CARs have been shown in Table 2. Overall, CARM's results are characterized by two distinct features: mutual association between RIFs and high correlation with reality. Firstly, mutual association can be found in four of the Top 10 CARs, such as the No.1 and the No.8, the No.2 and the No.3, i.e., there is a bi-directional association rule between M7 (drill) and M6 (training) and SE (engine power) and SG (gross tonnage). From a perspective of reality, these mutual associations are highly credible. For example, both M7 (drill) and M6 (training) are necessary activities to upgrade the skills of crew members and familiarise them with emergency procedures and action plans to avoid marine accidents from occurring or evolving into more serious ones. They have a close and complementary relationship with each other. Similarly, although there is a complex and indirect linear relationship between SE (engine power) and SG (gross tonnage), for the most cases, if a ship has a larger size, it also needs more propulsive power, i.e. higher main engine power, to achieve the required speed. Therefore, the reality scenario validates the strong association relationships between these two RIFs, as well as the effectiveness of this method.

Furthermore, more illustrations can be found in Table 2. For example, ES (sea state, represented in the dataset by local wave conditions) and EC (current speed) may co-occur in accident records because both characterize the local hydrodynamic environment encountered by a vessel. Previous wave–current interaction studies have shown that ambient currents can modify local wave propagation, slope, and steepness [53,54]; H2 (education and training) contributes to the accumulation and development of H3 (experience) [55]; M5 (company safety culture) is the collection of safety priorities, practices, beliefs, policies and behaviors in an organisation, which is embedded at every level of the company and is a key factor in the success of M3 (safety management system) [55]; M1 (regulation) is the framework, criteria and orientation of M2 (supervision), which ensures the effectiveness and fairness of supervision. As a result, a high level of association and uncertainty can be identified between the different RIFs in the development of marine accidents. Further exploration of these coupling effect through a topological and quantitative lens provides additional insights into the prevention and evolution of marine accidents.

### 3.2. Causality analysis of influential factors based on DEMATEL

The CARM derived direct influence matrix was normalized using Eqs. (3) and (4), yielding the normalized influence matrix *NorG*. Eq. (5) was then used to obtain the comprehensive influence matrix *T*. Based on *T*, the influence degree I, influenced degree *BI*, centrality degree *CE*, cause degree *CA*, and weight *WE* were calculated using Eqs. (6)–(10). The corresponding matrix and indicator values are reported in Tables 3 and 4.

Utilizing the DEMATEL method, the centrality degree reveals the central position and impact of the RIFs within the occurrence of marine accidents; the cause distinguishes whether a RIF acts as an originator or a recipient of influence; and the weight reflects the comparative importance of each RIF. Collectively, these indicators provide insights into the intricate dynamics among RIFs during the progression of marine accidents, thereby facilitating more informed and efficacious decision-making. Specifically, the causal distribution of the RIFs is plotted by the values of CE and CA; the corresponding distribution appears in Fig. 2. The descending centrality order is SE (engine power; 2.4820), SG (gross tonnage; 2.4714), M6 (training; 2.4045), M7 (drill; 2.3386), and M5 (company safety culture; 2.2832). Furthermore, Fig. 3 presents the weight distribution of RIFs. From Fig. 3, SE (engine power), SG (gross tonnage), M6 (training), M7 (drill) and M3 (safety management system) rank the highest in terms of weight values, corroborating a positive relationship with centrality findings. Notably, among these factors, SE

**Table 2**
Top 10 CARs ranked by conviction values.

| No. | Antecedent | Consequent | CC | No. | Antecedent | Consequent | CC |
|---|---|---|---|---|---|---|---|
| 1 | M7 | M6 | 10.13 | 6 | M5 | M3 | 7.41 |
| 2 | SE | SG | 9.44 | 7 | M1 | M2 | 6.54 |
| 3 | SG | SE | 9.30 | 8 | M6 | M7 | 5.17 |
| 4 | ES | EC | 9.14 | 9 | SV1 | SV3 | 4.69 |
| 5 | H2 | H3 | 8.49 | 10 | ST | SG | 4.55 |

**Table 3**
The calculated result of comprehensive influence matrix.

| RIFs | H1 | H2 | H3 | H4 | H5 | H6 | … … | ES | EC | ET | ED | AT | T |
|---|---|---|---|---|---|---|---|---|---|---|---|---|---|
| H1 | 0.0090 | 0.0250 | 0.0291 | 0.0212 | 0.0336 | 0.0337 | … … | 0.0050 | 0.0085 | 0.0240 | 0.0243 | 0.0246 | 0.0242 |
| H2 | 0.0290 | 0.0174 | 0.1336 | 0.0266 | 0.0576 | 0.0447 | … … | 0.0083 | 0.0269 | 0.0294 | 0.0390 | 0.0317 | 0.0307 |
| H3 | 0.0243 | 0.0320 | 0.0155 | 0.0225 | 0.0392 | 0.0355 | … … | 0.0058 | 0.0098 | 0.0254 | 0.0289 | 0.0254 | 0.0249 |
| H4 | 0.0279 | 0.0336 | 0.0692 | 0.0098 | 0.0522 | 0.0477 | … … | 0.0060 | 0.0092 | 0.0331 | 0.0282 | 0.0321 | 0.0260 |
| H5 | 0.0241 | 0.0267 | 0.0308 | 0.0220 | 0.0156 | 0.0394 | … … | 0.0067 | 0.011 | 0.0253 | 0.0267 | 0.0263 | 0.0252 |
| H6 | 0.0241 | 0.0262 | 0.0307 | 0.0219 | 0.0457 | 0.0135 | … … | 0.0060 | 0.0010 | 0.0249 | 0.0258 | 0.0252 | 0.0248 |
| … … | … … | … … | … … | … … | … … | … … | … … | … … | … … | … … | … … | … … | … … |
| ES | 0.0063 | 0.0101 | 0.0086 | 0.0058 | 0.0105 | 0.0085 | … … | 0.0097 | 0.1364 | 0.0068 | 0.0261 | 0.0348 | 0.0248 |
| EC | 0.0078 | 0.0234 | 0.0117 | 0.0064 | 0.0124 | 0.0106 | … … | 0.0256 | 0.0133 | 0.0078 | 0.0246 | 0.0282 | 0.0241 |
| ET | 0.0211 | 0.0226 | 0.0256 | 0.0199 | 0.0264 | 0.0248 | … … | 0.0047 | 0.0078 | 0.0082 | 0.0232 | 0.0224 | 0.0222 |
| ED | 0.0242 | 0.0312 | 0.0379 | 0.0225 | 0.0357 | 0.0295 | … … | 0.0213 | 0.0273 | 0.0273 | 0.0136 | 0.0279 | 0.0267 |
| AT | 0.0243 | 0.0269 | 0.0294 | 0.0223 | 0.0325 | 0.0284 | … … | 0.0245 | 0.0338 | 0.0261 | 0.0283 | 0.0133 | 0.0269 |
| T | 0.0239 | 0.0263 | 0.0287 | 0.0216 | 0.0290 | 0.0277 | … … | 0.0209 | 0.0269 | 0.0253 | 0.0266 | 0.0270 | 0.0118 |

**Table 4**
The result of topological indicators of RIFs.

| RIFs | I | BI | CE | CA | Weight | Rank | RIFs | I | BI | CE | CA | Weight | Rank |
|---|---|---|---|---|---|---|---|---|---|---|---|---|---|
| H1 | 0.6833 | 0.66340 | 1.3472 | 0.0193 | 0.0233 | 27 | M2 | 0.9072 | 1.0524 | 1.9596 | -0.1452 | 0.0340 | 12 |
| H2 | 1.1244 | 0.8347 | 1.9591 | 0.2897 | 0.0343 | 11 | M3 | 0.8274 | 1.4069 | 2.2343 | -0.5795 | 0.0400 | 5 |
| H3 | 0.7749 | 1.0107 | 1.7855 | -0.2358 | 0.0312 | 16 | M4 | 0.8633 | 1.0161 | 1.8794 | -0.1528 | 0.0327 | 15 |
| H4 | 0.8119 | 0.5567 | 1.3686 | 0.2553 | 0.0241 | 26 | M5 | 1.0944 | 1.1889 | 2.2832 | -0.0945 | 0.0396 | 7 |
| H5 | 0.8218 | 1.0614 | 1.8832 | -0.2395 | 0.0329 | 14 | M6 | 1.0218 | 1.3827 | 2.4045 | -0.3609 | 0.0421 | 3 |
| H6 | 0.7806 | 0.9255 | 1.7061 | -0.1449 | 0.0297 | 20 | M7 | 1.1336 | 1.2050 | 2.3386 | -0.0713 | 0.0405 | 4 |
| ST | 1.0526 | 0.8550 | 1.9076 | 0.1976 | 0.0332 | 13 | EL | 0.8612 | 0.8850 | 1.7462 | -0.0238 | 0.0302 | 19 |
| SA | 0.8531 | 0.8574 | 1.7105 | -0.0043 | 0.0296 | 21 | EV | 0.6323 | 0.6044 | 1.2367 | 0.0279 | 0.0214 | 31 |
| SG | 1.0808 | 1.3906 | 2.4714 | -0.3098 | 0.0431 | 2 | EW | 0.8249 | 0.7755 | 1.6004 | 0.0494 | 0.0277 | 25 |
| SE | 1.0886 | 1.3934 | 2.4820 | -0.3048 | 0.0433 | 1 | ES | 0.7397 | 0.5006 | 1.2404 | 0.2391 | 0.0219 | 24 |
| SV1 | 1.3865 | 0.8446 | 2.2312 | 0.5419 | 0.0398 | 6 | EC | 0.7134 | 0.9132 | 1.6267 | -0.1998 | 0.0284 | 29 |
| SV2 | 1.2467 | 0.8573 | 2.1040 | 0.3894 | 0.0371 | 9 | ET | 0.5854 | 0.6691 | 1.2545 | -0.0837 | 0.0218 | 30 |
| SV3 | 1.2744 | 0.9399 | 2.2143 | 0.3346 | 0.0388 | 8 | ED | 0.9029 | 0.8768 | 1.7797 | 0.0262 | 0.0308 | 17 |
| SV4 | 0.9284 | 0.7628 | 1.6912 | 0.1656 | 0.0294 | 22 | AT | 0.8881 | 0.8770 | 1.7651 | 0.0110 | 0.0306 | 18 |
| SV5 | 0.6694 | 0.6633 | 1.3327 | 0.0062 | 0.0231 | 28 | T | 0.8345 | 0.8286 | 1.6631 | 0.0059 | 0.0288 | 23 |
| M1 | 1.2368 | 0.8453 | 2.0821 | 0.3916 | 0.0367 | 10 | | | | | | | |

Note: Rank indicates the order of the factors' weights

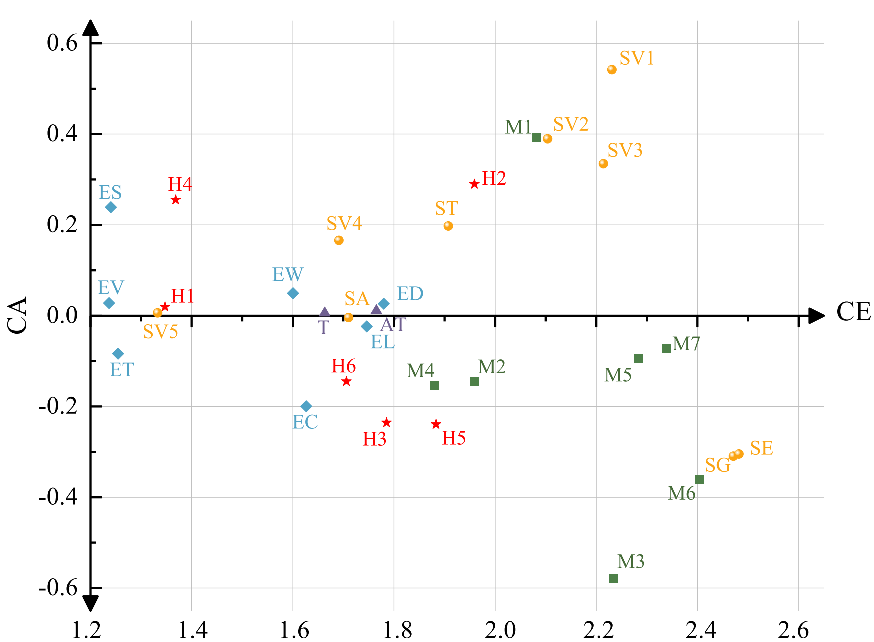


**Fig. 2.** The causal distribution of influential factors.

(engine power) and SG (gross tonnage) are ship factors, and M3 (safety management system), M5 (company safety culture), M6 (training) and M7 (drill) are management factors. This emphasizes the multifaceted influences on marine accidents from both ship and management perspectives. Accordingly, the management-related findings support strengthening safety-management implementation, company safety culture, crew training, and emergency drills, whereas the operational risks associated with engine power and gross tonnage should be

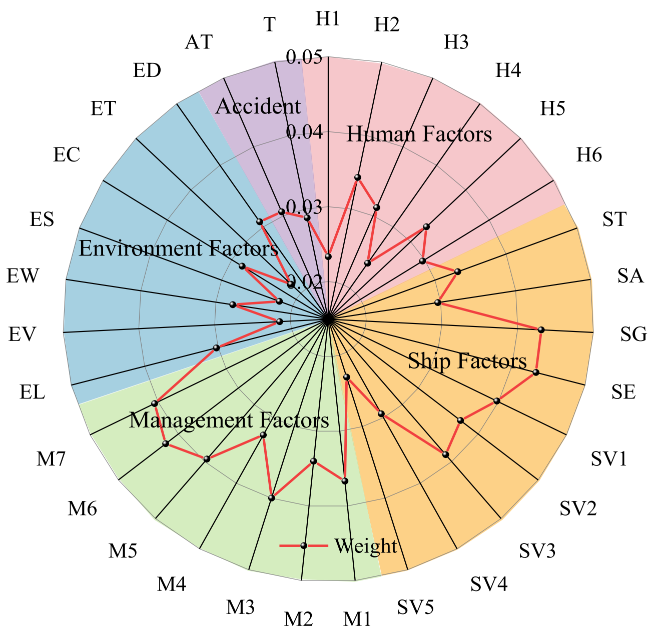


**Fig. 3.** The weight distribution of influential factors.

addressed through vessel-specific operating plans and appropriate safety margins.

In addition, *CA* offers additional perspectives on the roles of various RIFs. When $CA > 0$, it indicates that the RIF is a cause factor that exerts influence, while when $CA < 0$, the RIF is a result factor that is influenced by others. According to Table 4 and Fig. 2, RIFs like SV1 (ship certificates), M1 (regulation), SV2 (manning), SV3 (seafarer certificates) all exhibit *CA* values above zero, signifying their dominant influence on other factors [35]. By contrast, SE (engine power), SG (gross tonnage), M6 (training), and M3 (safety management system) all have negative *CA* values, indicating that their total incoming influence exceeds their total outgoing influence in the aggregated DEMATEL network. For M6 and M3, this suggests a stronger dependence on upstream organisational conditions; for SE and SG, which are fixed vessel descriptors, it reflects how their recorded categories are statistically embedded in combinations of ship type, vessel configuration, and operating context across accident records.

Taken together, factors with high centrality and negative cause occupy highly connected receiver-side positions in the aggregated network, including SE (engine power), SG (gross tonnage), and M6 (training). For M6, the negative net-cause value may reflect dependence on upstream organisational conditions. For SE and SG, however, the result should be interpreted only as a statistical link across accident records; it does not indicate that the installed engine power or gross tonnage of a vessel changes in response to other factors. Their practical relevance lies in managing the operating constraints associated with a given vessel through vessel-specific planning and appropriate safety margins. Similarly, factors with both high centrality and positive cause act as key influencers and drivers in accident occurrences, such as H2 (education and training), SV1 (ship certificates), M1 (regulation), SV2 (manning), and SV3 (seafarer certificates). These factors could serve as initial triggers that act in different ways before an accident occurs and potentially propagating adverse effects throughout the ship. For instance, issues related to certifications and manning, represented by SV1 (ship certificates), SV2 (manning), and SV3 (seafarer certificates), pose significant risks during voyages and may impede emergency responses, thereby facilitating the onset of accidents.

### *3.3. Hierarchical structure analysis of influential factors based on MMDE-WTAISM*

Based on the DEMATEL comprehensive influence matrix, MMDE-WTAISM was used to derive the downstream hierarchical relationship structure among the 31 RIFs. The MMDE-optimal candidate boundary was $k^* = 121$, corresponding to a threshold of 0.038319045145. Under the strict retention criterion $t_{ij} > \lambda_{\mathrm{MMDE}}$, 120 direct relationships were retained, and Boolean transitive closure subsequently produced 258 reachable relationships in the final reachability matrix, as shown in Table 5. The UP-type and DOWN-type computational extraction processes are detailed in Appendix B. Subsequently, the MMDE-WTAISM skeleton relationship structure was developed to clarify the connections among RIFs and computational levels. Tarjan's algorithm identified two non-singleton strongly connected components. The first SCC includes H5 (operational error), H6 (violation operation), the six management factors M2–M7, SE (engine power), and SG (gross tonnage), reflecting an operational–management–ship-condition feedback cluster. The second SCC consists of SV1 (ship certificate), SV2 (manning), and SV3 (seafarer certificates), indicating a certification-and-manning cluster related to vessel compliance and seaworthiness. These SCCs should therefore be interpreted as feedback groups rather than isolated single-cause factors.

In addition to the binary reachability structure, MMDE-WTAISM preserves DEMATEL-derived influence intensity through the weighted relationship matrix. As summarized in Table 6, the five highest weighted driving power (WDP) values are observed for SV1 (ship certificate), SV3 (seafarer certificates), SV2 (manning), M1 (regulation), and H2 (education and training). This indicates that certification, manning, regulatory, and competence-related factors exert strong retained downstream influence in the MMDE-WTAISM structure. In terms of weighted comprehensive importance (WCI), the leading factors are SV1 (ship certificate), M5 (company safety culture), M6 (training), M3 (safety management system), and SE (engine power), suggesting that these RIFs are not only structurally embedded in the retained relationship network but also highly involved in weighted influence exchanges. These weighted indicators provide complementary evidence beyond the binary hierarchy: SV1, SV3, and SV2 act as strong weighted drivers, whereas management and ship-condition factors occupy highly involved positions in the weighted interaction structure.

In this study, Figs. 4 and 5 present the UP-type and DOWN-type computational hierarchies obtained using MMDE-WTAISM. The results generated four computational hierarchical levels, which were further interpreted through three functional strata for risk-management purposes: the surface stratum corresponds to Level 1, the transitional stratum combines Levels 2 and 3, and the substantive stratum corresponds to Level 4. In the surface stratum, both the UP-type and DOWN-type hierarchies identify H5 (operational error), H6 (violation operation), the six management factors M2–M7, SE (engine power) and SG (gross tonnage). This common set overlaps with the first SCC, indicating that operational behaviour, management control, training/drill arrangements, and ship-condition factors form a closely coupled surface feedback cluster. This interpretation is consistent with recent maritime safety studies showing that safety climate, safety management, and unsafe seafarer behaviours are closely associated with crew safety awareness and onboard conduct [56,55]. The weighted results further support this interpretation, as M5, M6, M3, and SE are among the top five WCI factors. Thus, several surface-stratum factors are not merely located near the observable accident-response layer but are also highly involved in retained weighted influence exchanges. The UP-type hierarchy additionally places AT (accident type), EC (current speed), EL (location), ET (traffic density), H1 (physical and psychological state), SA (ship age), SV5 (PSC/FSC inspection), and T (time) in the surface stratum, suggesting that accident-context, environmental, ship-age, inspection, and temporal factors become more directly visible under the UP-type extraction perspective. This finding is also compatible with

**Table 5**
The MMDE-WTAISM reachability matrix of the RIFs.

| RIF | H1 | H2 | H3 | H4 | H5 | H6 | … | ES | EC | ET | ED | AT | T |
|---|---|---|---|---|---|---|---|---|---|---|---|---|---|
| H1 | 1 | 0 | 0 | 0 | 0 | 0 | … | 0 | 0 | 0 | 0 | 0 | 0 |
| H2 | 0 | 1 | 1 | 0 | 1 | 1 | … | 0 | 0 | 0 | 1 | 0 | 0 |
| H3 | 0 | 0 | 1 | 0 | 1 | 1 | … | 0 | 0 | 0 | 0 | 0 | 0 |
| H4 | 0 | 0 | 1 | 1 | 1 | 1 | … | 0 | 0 | 0 | 0 | 0 | 0 |
| H5 | 0 | 0 | 0 | 0 | 1 | 1 | … | 0 | 0 | 0 | 0 | 0 | 0 |
| H6 | 0 | 0 | 0 | 0 | 1 | 1 | … | 0 | 0 | 0 | 0 | 0 | 0 |
| … | … | … | … | … | … | … | … | … | … | … | … | … | … |
| ES | 0 | 0 | 0 | 0 | 0 | 0 | … | 1 | 1 | 0 | 0 | 0 | 0 |
| EC | 0 | 0 | 0 | 0 | 0 | 0 | … | 0 | 1 | 0 | 0 | 0 | 0 |
| ET | 0 | 0 | 0 | 0 | 0 | 0 | … | 0 | 0 | 1 | 0 | 0 | 0 |
| ED | 0 | 0 | 0 | 0 | 1 | 1 | … | 0 | 0 | 0 | 1 | 0 | 0 |
| AT | 0 | 0 | 0 | 0 | 0 | 0 | … | 0 | 0 | 0 | 0 | 1 | 0 |
| T | 0 | 0 | 0 | 0 | 0 | 0 | … | 0 | 0 | 0 | 0 | 0 | 1 |

**Table 6**
Top five RIFs ranked by weighted driving power and weighted comprehensive importance.

| Rank | RIF by WDP | WDP | RIF by WCI | WCI |
|---|---|---|---|---|
| 1 | SV1 | 0.945924 | SV1 | 1.047763 |
| 2 | SV3 | 0.734118 | M5 | 1.045842 |
| 3 | SV2 | 0.733346 | M6 | 1.034140 |
| 4 | M1 | 0.581321 | M3 | 1.030942 |
| 5 | H2 | 0.549444 | SE | 0.974147 |

accident-severity research reporting associations between marine accident severity and AT, SE, SG, ST, and EL [14].

The transitional functional stratum bridges the surface and substantive strata and corresponds to computational Levels 2 and 3. Both the UP-type and DOWN-type hierarchies identify ED (depth-draft ratio), H3 (experience), EW (wind force), H2 (education and training), and M1 (regulation) within this stratum. These common transitional RIFs can be interpreted as intermediate transmission factors linking navigational constraints, crew competence, meteorological exposure, and regulatory conditions with more visible operational and management responses. Earlier accident-severity research indicates that deficiencies in vessel certification, crew complement, or seafarer credentials may be associated with a greater likelihood of severe marine-accident outcomes [31]. Weighted results reinforce this interpretation, as SV1, SV3, and SV2 rank as the three highest WDP factors, indicating that regulatory conditions and education-and-training capacity are not only transitional links but also strong retained weighted drivers. In the UP-type hierarchy, EV (visibility), ST (ship type), SV4 (seaworthiness), ES (sea state), and H4 (communication) additionally appear in the transitional stratum, whereas the DOWN-type hierarchy additionally identifies EC (current speed) and ET (traffic density). This direction-dependent position suggests that EC can be operationally visible under the UP-type extraction while acting as an intermediate factor under the DOWN-type extraction, and its practical relevance should therefore be interpreted primarily in navigational accident contexts, such as collisions, groundings, and contacts. More broadly, environmental, vessel-condition, communication, hydrodynamic, and traffic-exposure factors may occupy different transmission positions depending on the extraction perspective [25].

The substantive functional stratum corresponds to computational Level 4 and represents deeper boundary-condition or long-term governance-related RIFs in the hierarchical interpretation. Both hierarchies identify SV1 (ship certificate), SV2 (manning), and SV3 (seafarer certificates) within this stratum. This shared certification-and-manning set is consistent with the second SCC and indicates that vessel documentation, crew sufficiency, and seafarer qualification form a stable foundation for the downstream MMDE-WTAISM structure. Earlier accident-severity research indicates that deficiencies in vessel certification, crew complement, or seafarer credentials may be associated with a greater likelihood of severe marine-accident outcomes [31]. Weighted results reinforce this interpretation, as SV1, SV3, and SV2 rank as the three highest WDP factors, indicating that the substantive certification-and-manning cluster exerts the strongest retained downstream weighted influence. Under the DOWN-type extraction perspective, the substantive stratum is broader and further includes AT (accident type), EL (location), ES (sea state), EV (visibility), H1 (physical and psychological state), H4 (communication), SA (ship age), ST (ship type), SV4 (seaworthiness), SV5 (PSC/FSC inspection), and T (time). These additional factors suggest that accident-context, environmental, human-condition, vessel-characteristic, inspection-related, and

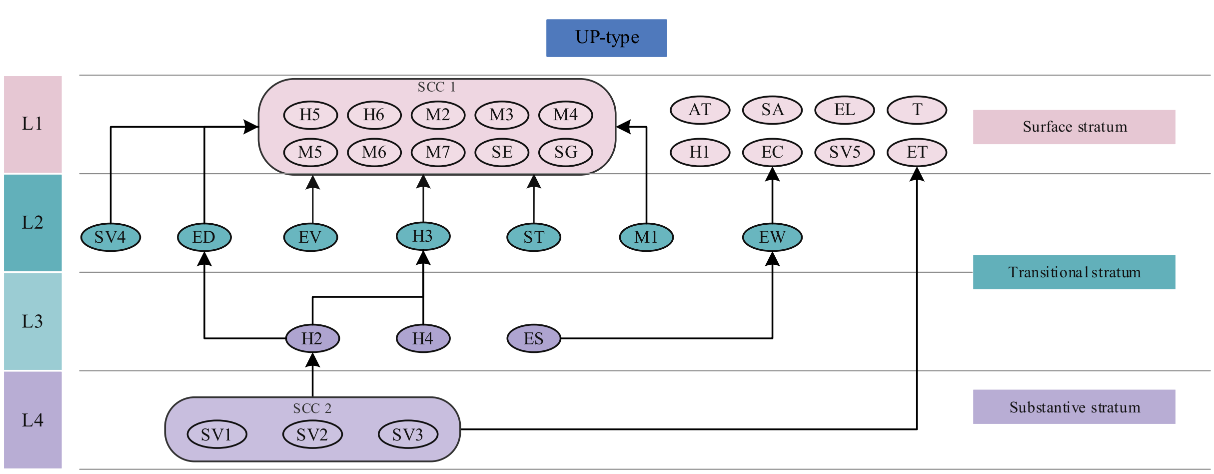


**Fig. 4.** The result of UP-type topological hierarchical structure.

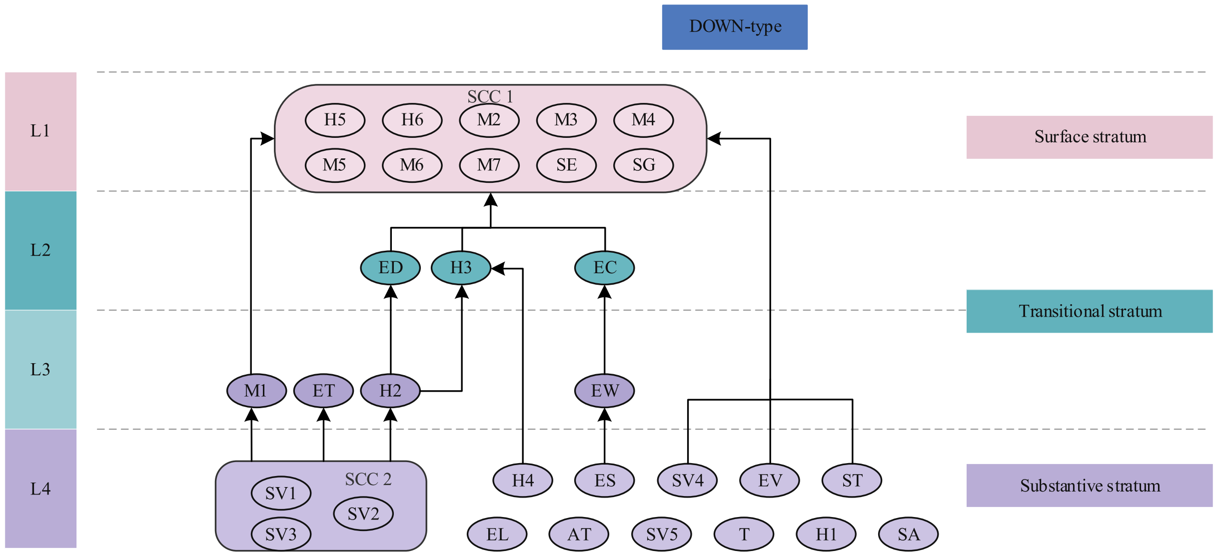


**Fig. 5.** The result of DOWN-type topological hierarchical structure.

temporal conditions may serve as deeper boundary conditions under the reverse hierarchical interpretation.

### 3.4. Sampling uncertainty and stability of key results

Sampling uncertainty was evaluated by a non-parametric case-resampling bootstrap. In each of 1,000 replicates, 1,294 complete accident records were sampled with replacement, and the full CARM-DEMATEL-MMDE-WTAISM sequence was re-estimated using the same analytical settings. All replicates completed successfully. Module-level stability was evaluated using the number of factor-level CARs, rank correlation of the DEMATEL comprehensive influence matrix, recurrence of MMDE-retained direct relationships, SCC co-membership, agreement of WTAISM functional strata, and rank correlation of the weighted indicators. The resulting measures are summarized in Table 7.

The association and influence components were highly reproducible: the CARM rule yield remained close to the full-sample value of 826, and the DEMATEL influence ordering had a mean rank correlation of 0.945. For MMDE, the median recurrence of the 120 full-sample direct relationships was 0.988, indicating that sampling variation primarily affected links close to the adaptive boundary. WTAISM conclusions were more stable at the functional-stratum level than at the exact computational-level position. The management interpretation therefore relies on the surface, transitional, and substantive strata rather than treating every four-level node position as invariant. The SV1-SV2-SV3 feedback component was nearly invariant internally, whereas the larger SCC retained a recurrent core with a more sample-sensitive boundary.

The weighted-indicator rankings were also highly stable, with mean rank correlations of 0.935 for WDP and 0.948 for WCI. This indicates that the full-sample weighted rankings reported in Table 6 were broadly preserved across the bootstrap replicates. In the full sample, the five highest WDP values were observed for SV1, SV3, SV2, M1, and H2, whereas the five highest WCI values were observed for SV1, M5, M6, M3, and SE. Accordingly, certification, manning, competence, regulation, and safety-management deficiencies warrant sustained preventive attention, whereas engine power should inform vessel-specific planning and operational margins rather than be treated as a directly controllable risk condition.

**Table 7**
Bootstrap stability of the CARM-DEMATEL-MMDE-WTAISM framework.

| Framework component | Stability measure | Bootstrap result |
|---|---|---|
| CARM | Number of factor-level CARs | Mean 826.6; 95% PI 802-852 |
| DEMATEL | Rank correlation of off-diagonal elements of T | Mean 0.945; 95% PI 0.907-0.971 |
| MMDE relationship screening | Recurrence of the 120 full-sample direct relationships | Median 0.988; 78.3% recurred in at least 80% of replicates |
| SCC structure | Within-component pairwise co-membership | SV1-SV2-SV3: 0.998; 10-member SCC: 0.759 |
| WTAISM hierarchy | Agreement of functional strata | UP: 0.750; DOWN: 0.733 |
| Weighted key-factor analysis | Rank correlation of weighted indicators | WDP: 0.935; WCI: 0.948 |

## 4. Discussion and implications

This section contains two parts, the theoretical and practical implications of the findings in Sections 4.1 and 4.2, respectively.

### 4.1. Theoretical implications

Based on the results in Section 3, the novel data-driven framework proposed in this study facilitates both interrelationship and hierarchical analysis between marine accident RIFs. The interplay among the three methodologies discussed in Section 3 is further verified by the empirical findings, showcasing a notable coherence. For example, several high-ranking associations identified by CARM are reflected in the feedback clusters and weighted-indicator rankings obtained from MMDE-WTAISM. Using the CARM results as input data for DEMATEL, the topological indicators in Table 4 show that SE (engine power), SG (gross tonnage), and management factors (M1–M7) occupy highly connected positions in the aggregated RIF network. Here, SE represents installed engine power and serves as an indicator of vessel propulsion capability, whereas SG denotes gross tonnage, a standardized, volume-based measure of vessel size derived from the volume of its enclosed spaces. As fixed vessel descriptors, SE and SG should not be interpreted as direct causes of accidents or as quantities that are changed by other RIFs. Rather, their high network prominence indicates that particular engine-power and gross-tonnage categories are repeatedly connected with operational, environmental, and management conditions in the aggregated accident network. By contrast, factors whose relevance is concentrated in narrower operational contexts may occupy less prominent positions in the aggregated network because pooling heterogeneous accident and ship types can dilute scenario-specific associations. For example, visibility, traffic density, and the physical and psychological condition of operators may become particularly important in restricted-visibility, congested-waterway, or human-performance-related scenarios, even when their overall connectivity across the full dataset is comparatively limited. The resulting rankings should therefore be interpreted as measures of dataset-wide network connectivity rather than as a universal ordering of practical importance across all accident scenarios. This network-based interpretation is broadly consistent with previous studies on marine accident severity and risk-factor modelling [14], providing external support for the plausibility of the proposed framework.

As an innovative extension of the ARM technique, this study develops the CARM method, aimed at overcoming the limitations of traditional ARM approaches which typically only discern association rules between different states rather than in the factor level. As a data-driven machine learning method, CARM uncovers hidden and intricate relationships at the factor level, accommodating association rules across both binary and multivariate variables. For example, M6 (Training) is a binary variable, i.e., 'Yes' for inadequate training and 'No' for adequate training, while ST (Ship Types) encompasses ten distinct types, each representing a different state (from ST1 to ST10). If there is an association rule between M6 and ST, the conventional ARM may only recognize the association relationship from 'No' to ST1, where the results of ARM involving such binary states (yes or no) are unclear. However, CARM multiplies the conviction by the probability of each rule, and then reveals the association rules between the factors by summing the estimated mathematical expectation. Therefore, CARM serves as the data-driven basis for mining factor-level combined association rules from marine accident data, thereby reducing reliance on subjective expert judgement. However, this method has certain limitations. For instance, the combined association rules obtained through expectation-based CC calculation may overlook the distribution characteristics of association strength at the state level and could be influenced by extreme values, resulting in the loss of some critical information. Nevertheless, this study has mitigated the impact of extremely low-probability events by setting an appropriate support threshold to minimize their interference with the analysis results.

DEMATEL serves as a method for exploring the interaction and causal relationships between factors [19]. Distinct from other method such as CNs, which tends to focus on static topological relationships among factors (Feng et al., 2024a), DEMATEL takes a step further by elucidating the causal links between these RIFs. In the study of marine accidents, it will be more theoretically significant to reveal the causal relationships. Thus, CARM provides a quantitative method for discovering associations from large amounts of data, while DEMATEL translates these association rules into a comprehensive matrix that highlights the causal interplay among factors. This integration of methods allows a fusion of data-driven insights with a nuanced qualitative understanding of marine accidents.

Furthermore, this study develops an MMDE-based weighted extension of TAISM as the downstream structural interpretation module. In conjunction with DEMATEL, MMDE-WTAISM replaces the original empirical thresholding rule with an MMDE-derived adaptive threshold and preserves DEMATEL-derived influence intensity through a weighted relationship matrix. Based on the MMDE-WTAISM reachability structure, strongly connected components identify mutually reachable feedback groups, supporting the interpretation of coupled RIF clusters rather than isolated single factors. Across computational levels, MMDE-WTAISM clarifies the hierarchical positions of RIFs and supports the interpretation of potential transmission pathways among surface, transitional, and substantive functional strata. Compared with fixed expert-weighting hierarchies such as AHP, the proposed framework updates the downstream hierarchy through data-driven relationship screening and weighted influence preservation when new accident information becomes available. Therefore, the integrated application of these methods furnishes a robust and dynamic theoretical framework for the identification and analysis of RIFs in marine accidents, offering significant advancements at the theoretical level.

### 4.2. Practical implications

From a practical perspective, the hierarchical relationship analysis in this study provides a structured approach for exploring the influence mechanism and correlations among marine accident RIFs. The MMDE-WTAISM results generate four computational hierarchical levels, which are further aggregated into surface, transitional, and substantive functional strata for risk-management interpretation. In the substantive functional stratum, SV1 (ship certificate), SV2 (manning), and SV3 (seafarer certificates) represent long-term certification-and-manning governance priorities. These factors are also the top three weighted driving-power factors, suggesting that vessel documentation, crew sufficiency, and seafarer qualification have strong retained downstream influence in the weighted relationship structure. By contrast, M1 (regulation) and H2 (education and training) are located in the transitional functional stratum and also rank among the top five weighted driving-power factors, indicating that regulatory conditions and education-and-training capacity may serve as both intermediate transmission factors and important weighted drivers. At the surface functional stratum, H5 (operational error), H6 (violation operation), the six management factors M2–M7, SE (engine power), and SG (gross tonnage) form a structurally prominent feedback group.

Compared with studies that mainly propose general improvement measures after identifying important RIFs [60], the MMDE-WTAISM results provide a more structured basis for linking accident prevention, risk control, and emergency response. Based on the topological hierarchical structures presented in Section 3.3, long-term governance should prioritize certification validity, adequate manning, seafarer qualification, regulatory quality, and education-and-training capacity. At the operational level, shipping companies, shipboard operators, and relevant onboard departments should strengthen supervision, safety-management implementation, problem rectification, training, drills, and ship-condition-aware decision-making to identify and respond to risk signals before they escalate. For objective or intrinsic factors, such as current speed, engine power, and gross tonnage, practical intervention should focus on managing the associated operational risks rather than changing the factors themselves, for example through voyage planning, current forecasting, route adjustment, speed and course compensation, larger manoeuvring margins, and coordinated bridge–engine-room responses in confined or high-risk waters.

In summary, the practical implications of this study are not limited to ranking individual RIFs. Instead, the MMDE-WTAISM framework distinguishes weighted drivers, highly embedded factors, feedback clusters, and functional strata. Stakeholders can use the substantive stratum to design preventive and forward-looking strategies, the transitional stratum to monitor intermediate transmission factors, and the surface stratum to support immediate risk control and emergency response. In this way, the proposed framework may help maritime stakeholders interrupt or slow potential risk-propagation pathways while maintaining a long-term focus on systemic safety governance.

## 5. Conclusion

This study developed a CARM-DEMATEL-MMDE-WTAISM framework to analyse factor-level associations, data-derived influence roles, weighted relationships, and hierarchical structures among 31 marine accident RIFs.

First, CARM generated 826 directed factor-level combined association rules from 1,294 accident records. By aggregating state-level conviction evidence, CARM provides a quantitative input for subsequent influence analysis while reducing reliance on subjective expert scoring.

Second, the data-driven DEMATEL module quantified direct and indirect influence within the aggregated RIF network. SE, SG, M6, M7, and M5 had the highest centrality values, while SV1, M1, SV2, and SV3 showed positive net-cause characteristics. These findings describe global network roles across the dataset; they do not imply that intrinsic vessel attributes physically change in response to other factors.

Third, MMDE-WTAISM retained 120 direct relationships and produced 258 reachable relationships using an adaptive threshold of 0.038319045145. It identified two non-singleton strongly connected components (H5, H6, M2-M7, SE, and SG; and SV1-SV3), preserved DEMATEL-derived influence intensity through weighted indicators, and generated four-level UP-type and DOWN-type computational hierarchies. These levels were further interpreted as surface, transitional, and substantive functional strata.

The 1,000-replicate full-framework bootstrap showed that the key weighted rankings were highly reproducible (mean rank correlations of 0.935 for WDP and 0.948 for WCI), whereas exact four-level node placement and the boundary of the larger feedback component were more sample-sensitive. The conclusions should therefore emphasize persistent key-factor groups, recurrent feedback regions, and functional strata rather than invariant rank positions or component boundaries.

The combined results support layered risk governance. Certification validity, adequate manning, seafarer qualification, regulatory quality, and education-and-training capacity require sustained preventive attention. Intermediate environmental, competence, and regulatory conditions require monitoring, while the operational-management-ship-condition feedback region requires coordinated supervision and response.

This study offers valuable contributions from both theoretical and practical perspectives, however several issues remain, wanting future research to be conducted. Firstly, the findings presented are broad and applicable to a wide range of accidents and ship types; however, this study lacks a targeted analysis that differentiates between specific types of accidents and ship types. Secondly, the research primarily focuses on identifying RIFs at the system level, without considering the severity of the accidents. Future research could enhance the CARM technique by introducing weights that account for accident severity. Finally, although this study employs a novel data-driven approach, it does not quantify the impact of individual RIFs on accident outcomes. Future research could address this gap by applying more advanced techniques (such as causal inference) to quantify the specific effects of these risk factors on marine accidents.

## CRediT authorship contribution statement

**Yinwei Feng:** Writing – original draft, Methodology, Investigation, Data curation, Conceptualization. **Xinjian Wang:** Writing – original draft, Supervision, Methodology, Funding acquisition, Formal analysis, Conceptualization. **Yuhao Cao:** Writing – original draft, Visualization, Validation, Methodology, Investigation, Conceptualization. **Jingen Zhou:** Writing – review & editing, Validation, Resources, Formal analysis. **Jin Wang:** Writing – review & editing, Visualization, Supervision, Investigation, Formal analysis. **Zaili Yang:** Writing – review & editing, Validation, Supervision, Resources, Funding acquisition, Formal analysis.

## Declaration of competing interest

The authors declare that they have no known competing financial interests or personal relationships that could have appeared to influence the work reported in this paper.

## Acknowledgements

The authors gratefully acknowledge support from the Joint Project of Liaoning Provincial Science and Technology Program [Grant No. 2025-BSLH-058], the Fundamental Research Funds for the Central Universities [Grant No. 3132026122].

## Appendixes

Appendix A: The code of RIFs.

**Table A1**
The classification of RIFs.

| Category | Variable | RIF | State | Description |
|---|---|---|---|---|
| Human | Physical & psychological state | H1 | Yes | Have physical & psychological problem |
| | | | No | No physical & psychological problem |
| | Education and training | H2 | Yes | Insufficient education and training |
| | | | No | Sufficient education and training |
| | Experience | H3 | Yes | Lack experience |
| | | | No | Have experience |
| | Communication | H4 | Yes | Have communication problem |
| | | | No | No communication problem |
| | Operational error | H5 | Yes | Have operational error |
| | | | No | No operational error |
| | Violation operation | H6 | Yes | Violation of rules and regulations |
| | | | No | No violation of rules and regulations |
| Ship | Ship type | ST | ST1 | Bulk carrier |
| | | | ST2 | Container ship |
| | | | ST3 | Oil tanker |
| | | | ST4 | Passenger ship (including cruise and ro-ro passenger ship) |
| | | | ST5 | Chemical tanker |
| | | | ST6 | General cargo ship |
| | | | ST7 | Fishing vessel |
| | | | ST8 | Yacht and sailing vessel |
| | | | ST9 | Tug and port traffic boat |
| | | | ST10 | Others |
| | Ship age | SA | SA1 | 0-10 years |
| | | | SA2 | 10-20 years |
| | | | SA3 | 20-30 years |

(*continued on next page*)

**Table A1** (*continued*)

| Category | Variable | RIF | State | Description |
|---|---|---|---|---|
| | | | SA4 | ≥30 years |
| | Gross tonnage | SG | SG1 | <500t |
| | | | SG2 | 500-3000t |
| | | | SG3 | ≥3000t |
| | Engine power | SE | SE1 | <750KW |
| | | | SE2 | 750-3000KW |
| | | | SE3 | ≥3000KW |
| | Ship certificate | SV1 | Yes | Incomplete or invalid ship certificates |
| | | | No | Complete and valid ship certificates |
| | Manning | SV2 | Yes | Insufficient manning |
| | | | No | Sufficient manning |
| | Seafarer certificates | SV3 | Yes | Incomplete or invalid seafarer certificates |
| | | | No | Complete and valid seafarer certificates |
| | Seaworthiness | SV4 | Yes | Have seaworthiness problem |
| | | | No | No seaworthiness problem |
| | Port State Control/Flag State Control (PSC/FSC) inspection | SV5 | Yes | Defective ship |
| | | | No | Non-defective ship |
| Management | Regulation | M1 | Yes | Inadequate regulation |
| | | | No | Adequate regulation |
| | Supervision | M2 | Yes | Inadequate supervision |
| | | | No | Adequate supervision |
| | Safety management system | M3 | Yes | Defective safety management system |
| | | | No | Non-defective safety management system |
| | Rectification of problems | M4 | Yes | Unresponsive rectification of problem |
| | | | No | Responsive rectification of problem |
| | Company safety culture | M5 | Yes | Have company safety culture problem |
| | | | No | No company safety culture problem |
| | Training | M6 | Yes | Inadequate ship training |
| | | | No | Adequate ship training |
| | Drill | M7 | Yes | Unscheduled drills |
| | | | No | Scheduled drills |
| Environment | Location | EL | EL1 | Inland waters |
| | | | EL2 | Port |
| | | | EL3 | Coastal waters |
| | | | EL4 | Open sea |
| | Visibility | EV | EV1 | Poor visibility (0.5-2nm) |
| | | | EV2 | Very Poor(<0.5nm) |
| | | | EV3 | Others |
| | Wind force | EW | EW1 | Strong wind (6-7*) |
| | | | EW2 | Very strong wind (8-9) |
| | | | EW3 | Storm (10-12) |
| | | | EW4 | Others |
| | Sea State | ES | ES1 | Poor sea state |
| | | | ES2 | Very poor sea state |
| | | | ES3 | Others |
| | Current speed | EC | EC1 | Current speed ≥ 4kn |
| | | | EC2 | Current speed < 4kn |
| | Traffic density | ET | ET1 | Heavy traffic density |
| | | | ET2 | Low traffic density |
| | Depth-draft ratio (h/d) | ED | ED1 | h/d < 1.2 |
| | | | ED2 | 1.2 ≤ h/d < 1.5 |
| | | | ED3 | 1.5 ≤ h/d < 3 |
| | | | ED4 | h/d ≥ 3 |
| Accident information | Accident type | AT | AT1 | Collision |
| | | | AT2 | Stranding/Ground |
| | | | AT3 | Fire/Explosion |
| | | | AT4 | Contact |
| | | | AT5 | Capsize/Sinking |
| | | | AT6 | Hull/Machinery damage |
| | | | AT7 | Others |
| | Time | T | T1 | 0000-0400 |
| | | | T2 | 0400-0800 |
| | | | T3 | 0800-1200 |
| | | | T4 | 1200-1600 |
| | | | T5 | 1600-2000 |
| | | | T6 | 2000-2400 |

*Unit: Beaufort scale.

Appendix B: The UP-type and DOWN-type hierarchical processes

**Table B1**
First iterative extraction of the UP-type and DOWN-type hierarchies.

| RIF | UP-type RS | UP-type TS | DOWN-type QS | DOWN-type TS |
|---|---|---|---|---|
| H1 | H1 | H1 | H1 | H1 |
| H2 | H2, H3, H5, H6, SG, SE, M2, M3, M4, M5, M6, M7, ED | H2 | H2, SV1, SV2, SV3 | H2 |
| H3 | H3, H5, H6, SG, SE, M2, M3, M4, M5, M6, M7 | H3 | H2, H3, H4, SV1, SV2, SV3 | H3 |
| H4 | H3, H4, H5, H6, SG, SE, M2, M3, M4, M5, M6, M7 | H4 | H4 | H4 |
| H5 | H5, H6, SG, SE, M2, M3, M4, M5, M6, M7 | H5, H6, SG, SE, M2, M3, M4, M5, M6, M7 | H2, H3, H4, H5, H6, ST, SG, SE, SV1, SV2, SV3, SV4, M1, M2, M3, M4, M5, M6, M7, EV, ED | H5, H6, SG, SE, M2, M3, M4, M5, M6, M7 |
| H6 | H5, H6, SG, SE, M2, M3, M4, M5, M6, M7 | H5, H6, SG, SE, M2, M3, M4, M5, M6, M7 | H2, H3, H4, H5, H6, ST, SG, SE, SV1, SV2, SV3, SV4, M1, M2, M3, M4, M5, M6, M7, EV, ED | H5, H6, SG, SE, M2, M3, M4, M5, M6, M7 |
| ST | H5, H6, ST, SG, SE, M2, M3, M4, M5, M6, M7 | ST | ST | ST |
| SA | SA | SA | SA | SA |
| SG | H5, H6, SG, SE, M2, M3, M4, M5, M6, M7 | H5, H6, SG, SE, M2, M3, M4, M5, M6, M7 | H2, H3, H4, H5, H6, ST, SG, SE, SV1, SV2, SV3, SV4, M1, M2, M3, M4, M5, M6, M7, EV, ED | H5, H6, SG, SE, M2, M3, M4, M5, M6, M7 |
| SE | H5, H6, SG, SE, M2, M3, M4, M5, M6, M7 | H5, H6, SG, SE, M2, M3, M4, M5, M6, M7 | H2, H3, H4, H5, H6, ST, SG, SE, SV1, SV2, SV3, SV4, M1, M2, M3, M4, M5, M6, M7, EV, ED | H5, H6, SG, SE, M2, M3, M4, M5, M6, M7 |
| SV1 | H2, H3, H5, H6, SG, SE, SV1, SV2, SV3, M1, M2, M3, M4, M5, M6, M7, ET, ED | SV1, SV2, SV3 | SV1, SV2, SV3 | SV1, SV2, SV3 |
| SV2 | H2, H3, H5, H6, SG, SE, SV1, SV2, SV3, M1, M2, M3, M4, M5, M6, M7, ET, ED | SV1, SV2, SV3 | SV1, SV2, SV3 | SV1, SV2, SV3 |
| SV3 | H2, H3, H5, H6, SG, SE, SV1, SV2, SV3, M1, M2, M3, M4, M5, M6, M7, ET, ED | SV1, SV2, SV3 | SV1, SV2, SV3 | SV1, SV2, SV3 |
| SV4 | H5, H6, SG, SE, SV4, M2, M3, M4, M5, M6, M7 | SV4 | SV4 | SV4 |
| SV5 | SV5 | SV5 | SV5 | SV5 |
| M1 | H5, H6, SG, SE, M1, M2, M3, M4, M5, M6, M7 | M1 | SV1, SV2, SV3, M1 | M1 |
| M2 | H5, H6, SG, SE, M2, M3, M4, M5, M6, M7 | H5, H6, SG, SE, M2, M3, M4, M5, M6, M7 | H2, H3, H4, H5, H6, ST, SG, SE, SV1, SV2, SV3, SV4, M1, M2, M3, M4, M5, M6, M7, EV, ED | H5, H6, SG, SE, M2, M3, M4, M5, M6, M7 |
| M3 | H5, H6, SG, SE, M2, M3, M4, M5, M6, M7 | H5, H6, SG, SE, M2, M3, M4, M5, M6, M7 | H2, H3, H4, H5, H6, ST, SG, SE, SV1, SV2, SV3, SV4, M1, M2, M3, M4, M5, M6, M7, EV, ED | H5, H6, SG, SE, M2, M3, M4, M5, M6, M7 |
| M4 | H5, H6, SG, SE, M2, M3, M4, M5, M6, M7 | H5, H6, SG, SE, M2, M3, M4, M5, M6, M7 | H2, H3, H4, H5, H6, ST, SG, SE, SV1, SV2, SV3, SV4, M1, M2, M3, M4, M5, M6, M7, EV, ED | H5, H6, SG, SE, M2, M3, M4, M5, M6, M7 |
| M5 | H5, H6, SG, SE, M2, M3, M4, M5, M6, M7 | H5, H6, SG, SE, M2, M3, M4, M5, M6, M7 | H2, H3, H4, H5, H6, ST, SG, SE, SV1, SV2, SV3, SV4, M1, M2, M3, M4, M5, M6, M7, EV, ED | H5, H6, SG, SE, M2, M3, M4, M5, M6, M7 |
| M6 | H5, H6, SG, SE, M2, M3, M4, M5, M6, M7 | H5, H6, SG, SE, M2, M3, M4, M5, M6, M7 | H2, H3, H4, H5, H6, ST, SG, SE, SV1, SV2, SV3, SV4, M1, M2, M3, M4, M5, M6, M7, EV, ED | H5, H6, SG, SE, M2, M3, M4, M5, M6, M7 |
| M7 | H5, H6, SG, SE, M2, M3, M4, M5, M6, M7 | H5, H6, SG, SE, M2, M3, M4, M5, M6, M7 | H2, H3, H4, H5, H6, ST, SG, SE, SV1, SV2, SV3, SV4, M1, M2, M3, M4, M5, M6, M7, EV, ED | H5, H6, SG, SE, M2, M3, M4, M5, M6, M7 |
| EL | EL | EL | EL | EL |
| EV | H5, H6, SG, SE, M2, M3, M4, M5, M6, M7, EV | EV | EV | EV |
| EW | EW, EC | EW | EW, ES | EW |
| ES | EW, ES, EC | ES | ES | ES |
| EC | EC | EC | EW, ES, EC | EC |
| ET | ET | ET | SV1, SV2, SV3, ET | ET |
| ED | H5, H6, SG, SE, M2, M3, M4, M5, M6, M7, ED | ED | H2, SV1, SV2, SV3, ED | ED |
| AT | AT | AT | AT | AT |
| T | T | T | T | T |

In the first iteration, the UP-type procedure extracts Level 1 (AT, EC, EL, ET, H1, H5, H6, M2–M7, SA, SE, SG, SV5, and T), whereas the DOWN-type procedure extracts Level 4 (AT, EL, ES, EV, H1, H4, SA, ST, SV1–SV5, and T). After these factors are removed from their respective directional procedures, the remaining sets are recalculated.

**Table B2**
Second and third iterative extraction of the UP-type and DOWN-type hierarchies.

| UP-type RS | UP-type TS | DOWN-type QS | DOWN-type TS |
|---|---|---|---|
| H2, H3, ED | H2 | H2 | H2 |
| H3 | H3 | H2, H3 | H3 |
| H3, H4 | H4 | H2, H3, H5, H6, SG, SE, M1, M2, M3, M4, M5, M6, M7, ED | H5, H6, SG, SE, M2, M3, M4, M5, M6, M7 |
| ST | ST | H2, H3, H5, H6, SG, SE, M1, M2, M3, M4, M5, M6, M7, ED | H5, H6, SG, SE, M2, M3, M4, M5, M6, M7 |
| H2, H3, SV1, SV2, SV3, M1, ED | SV1, SV2, SV3 | H2, H3, H5, H6, SG, SE, M1, M2, M3, M4, M5, M6, M7, ED | H5, H6, SG, SE, M2, M3, M4, M5, M6, M7 |
| H2, H3, SV1, SV2, SV3, M1, ED | SV1, SV2, SV3 | H2, H3, H5, H6, SG, SE, M1, M2, M3, M4, M5, M6, M7, ED | H5, H6, SG, SE, M2, M3, M4, M5, M6, M7 |
| H2, H3, SV1, SV2, SV3, M1, ED | SV1, SV2, SV3 | M1 | M1 |
| SV4 | SV4 | H2, H3, H5, H6, SG, SE, M1, M2, M3, M4, M5, M6, M7, ED | H5, H6, SG, SE, M2, M3, M4, M5, M6, M7 |
| M1 | M1 | H2, H3, H5, H6, SG, SE, M1, M2, M3, M4, M5, M6, M7, ED | H5, H6, SG, SE, M2, M3, M4, M5, M6, M7 |
| EV | EV | H2, H3, H5, H6, SG, SE, M1, M2, M3, M4, M5, M6, M7, ED | H5, H6, SG, SE, M2, M3, M4, M5, M6, M7 |
| EW | EW | H2, H3, H5, H6, SG, SE, M1, M2, M3, M4, M5, M6, M7, ED | H5, H6, SG, SE, M2, M3, M4, M5, M6, M7 |
| EW, ES | ES | H2, H3, H5, H6, SG, SE, M1, M2, M3, M4, M5, M6, M7, ED | H5, H6, SG, SE, M2, M3, M4, M5, M6, M7 |
| ED | ED | H2, H3, H5, H6, SG, SE, M1, M2, M3, M4, M5, M6, M7, ED | H5, H6, SG, SE, M2, M3, M4, M5, M6, M7 |
| - | - | EW | EW |

(*continued on next page*)

**Table B2** (*continued*)

| UP-type RS | UP-type TS | DOWN-type QS | DOWN-type TS |
|---|---|---|---|
| - | - | EW, EC | EC |
| - | - | ET | ET |
| - | - | H2, ED | ED |
| H2 | H2 | H3 | H3 |
| H4 | H4 | H3, H5, H6, SG, SE, M2, M3, M4, M5, M6, M7, ED | H5, H6, SG, SE, M2, M3, M4, M5, M6, M7 |
| H2, SV1, SV2, SV3 | SV1, SV2, SV3 | H3, H5, H6, SG, SE, M2, M3, M4, M5, M6, M7, ED | H5, H6, SG, SE, M2, M3, M4, M5, M6, M7 |
| H2, SV1, SV2, SV3 | SV1, SV2, SV3 | H3, H5, H6, SG, SE, M2, M3, M4, M5, M6, M7, ED | H5, H6, SG, SE, M2, M3, M4, M5, M6, M7 |
| H2, SV1, SV2, SV3 | SV1, SV2, SV3 | H3, H5, H6, SG, SE, M2, M3, M4, M5, M6, M7, ED | H5, H6, SG, SE, M2, M3, M4, M5, M6, M7 |
| ES | ES | H3, H5, H6, SG, SE, M2, M3, M4, M5, M6, M7, ED | H5, H6, SG, SE, M2, M3, M4, M5, M6, M7 |
| - | - | H3, H5, H6, SG, SE, M2, M3, M4, M5, M6, M7, ED | H5, H6, SG, SE, M2, M3, M4, M5, M6, M7 |
| - | - | H3, H5, H6, SG, SE, M2, M3, M4, M5, M6, M7, ED | H5, H6, SG, SE, M2, M3, M4, M5, M6, M7 |
| - | - | H3, H5, H6, SG, SE, M2, M3, M4, M5, M6, M7, ED | H5, H6, SG, SE, M2, M3, M4, M5, M6, M7 |
| - | - | H3, H5, H6, SG, SE, M2, M3, M4, M5, M6, M7, ED | H5, H6, SG, SE, M2, M3, M4, M5, M6, M7 |
| - | - | H3, H5, H6, SG, SE, M2, M3, M4, M5, M6, M7, ED | H5, H6, SG, SE, M2, M3, M4, M5, M6, M7 |
| - | - | EC | EC |
| - | - | ED | ED |

In the second iteration, the UP-type procedure extracts Level 2 (ED, EV, EW, H3, M1, ST, and SV4), whereas the DOWN-type procedure extracts Level 3 (ET, EW, H2, and M1). In the third iteration, the UP-type procedure extracts Level 3 (ES, H2, and H4), whereas the DOWN-type procedure extracts Level 2 (EC, ED, and H3).

**Table B3**
Fourth iterative extraction of the UP-type and DOWN-type hierarchies.

| UP-type RS | UP-type TS | DOWN-type QS | DOWN-type TS |
|---|---|---|---|
| SV1, SV2, SV3 | SV1, SV2, SV3 | H5, H6, SG, SE, M2, M3, M4, M5, M6, M7 | H5, H6, SG, SE, M2, M3, M4, M5, M6, M7 |
| SV1, SV2, SV3 | SV1, SV2, SV3 | H5, H6, SG, SE, M2, M3, M4, M5, M6, M7 | H5, H6, SG, SE, M2, M3, M4, M5, M6, M7 |
| SV1, SV2, SV3 | SV1, SV2, SV3 | H5, H6, SG, SE, M2, M3, M4, M5, M6, M7 | H5, H6, SG, SE, M2, M3, M4, M5, M6, M7 |
| - | - | H5, H6, SG, SE, M2, M3, M4, M5, M6, M7 | H5, H6, SG, SE, M2, M3, M4, M5, M6, M7 |
| - | - | H5, H6, SG, SE, M2, M3, M4, M5, M6, M7 | H5, H6, SG, SE, M2, M3, M4, M5, M6, M7 |
| - | - | H5, H6, SG, SE, M2, M3, M4, M5, M6, M7 | H5, H6, SG, SE, M2, M3, M4, M5, M6, M7 |
| - | - | H5, H6, SG, SE, M2, M3, M4, M5, M6, M7 | H5, H6, SG, SE, M2, M3, M4, M5, M6, M7 |
| - | - | H5, H6, SG, SE, M2, M3, M4, M5, M6, M7 | H5, H6, SG, SE, M2, M3, M4, M5, M6, M7 |
| - | - | H5, H6, SG, SE, M2, M3, M4, M5, M6, M7 | H5, H6, SG, SE, M2, M3, M4, M5, M6, M7 |
| - | - | H5, H6, SG, SE, M2, M3, M4, M5, M6, M7 | H5, H6, SG, SE, M2, M3, M4, M5, M6, M7 |

In the fourth iteration, the UP-type procedure assigns SV1, SV2, and SV3 to Level 4, whereas the DOWN-type procedure assigns H5, H6, M2–M7, SE, and SG to Level 1.Table B2,B3 Table B4 summarizes the final computational levels.

**Table B4**
Final four-level UP-type and DOWN-type computational hierarchies.

| Computational level | UP-type RIFs | DOWN-type RIFs |
|---|---|---|
| L1 | AT, EC, EL, ET, H1, H5, H6, M2, M3, M4, M5, M6, M7, SA, SE, SG, SV5, T | H5, H6, M2, M3, M4, M5, M6, M7, SE, SG |
| L2 | ED, EV, EW, H3, M1, ST, SV4 | EC, ED, H3 |
| L3 | ES, H2, H4 | ET, EW, H2, M1 |
| L4 | SV1, SV2, SV3 | AT, EL, ES, EV, H1, H4, SA, ST, SV1, SV2, SV3, SV4, SV5, T |

## Data availability

Data will be made available on request.

## References


[1] United Nations Conference on Trade and Development. Review of maritime transport 2023. In: United Nations Conference on Trade and Development; 2023.
[2] Allianz Global Corporate & Specialty, 2022. Safety Shipping Review 2022. Allianz Global Corporate & Specialty, Munich.
[3] Wang J, Zhou Y, Zhuang L, Shi L, Zhang S. A model of maritime accidents prediction based on multi-factor time series analysis. J Mar Eng Technol 2023;22 (3):153–65. https://doi.org/10.1080/20464177.2023.2167269.
[4] Transportation Safety Board of Canada. Marine transportation occurrences in 2025. Transp Saf Board Can 2026.
[5] European Maritime Safety Agency. Annual overview of marine casualties and incidents 2025. Eur Marit Saf Agency 2025.
[6] Marine Accident Investigation Branch. Marine Accident Recommendations and Statistics. Mar Accid Investig Branch 2022.
[7] Fang S, Liu Z, Yang X, Wang X, Wang J, Yang Z. A quantitative study of the factors influencing human evacuation from ships. Ocean Eng 2023;285:115156. https://doi.org/10.1016/j.oceaneng.2023.115156.
[8] Ahmed U, Carpitella S, Certa A. An integrated methodological approach for optimising complex systems subjected to predictive maintenance. Reliab Eng Syst Saf 2021;216. https://doi.org/10.1016/j.ress.2021.108022.
[9] Xiao Z, Xie M, Wang X, Wang H, Fang S, Arnáez R. Risk assessment of emergency operations of floating storage and regasification unit. J Mar Eng Technol 2024;23 (5):357–72. https://doi.org/10.1080/20464177.2024.2364994.
[10] Wang X, Liu Z, Wang J, Loughney S, Zhao Z, Cao L. Passengers' safety awareness and perception of wayfinding tools in a Ro-Ro passenger ship during an emergency evacuation. Saf Sci 2021;137:105189. https://doi.org/10.1016/j.ssci.2021.105189.
[11] Li T, Wang X, Zhang Z, Feng Y. A novel feature engineering method for severity prediction of marine accidents. J Mar Eng Technol 2025:1–16. https://doi.org/10.1080/20464177.2025.2469336.
[12] Wang X, Yuan Y, Fang S, Zhang Z, Wang J. A novel causal inference method of exit choice behaviour analysis for passenger ships during emergency evacuation. Reliab Eng Syst Saf 2026;272:112489. https://doi.org/10.1016/j.ress.2026.112489.

[13] Zhou Y, Li C, Ding L, Sekula P, Love PED, Zhou C. Combining association rules mining with complex networks to monitor coupled risks. Reliab Eng Syst Saf 2019; 186:194–208. https://doi.org/10.1016/j.ress.2019.02.013.
[14] Cao Y, Wang X, Wang Y, Fan S, Wang H, Yang Z, Liu Z, Wang J, Shi R. Analysis of factors affecting the severity of marine accidents using a data-driven Bayesian network. Ocean Eng 2023;269. https://doi.org/10.1016/j.oceaneng.2022.113563.
[15] Guo M, Chen M, Yuan L, Zhang Z, Lv J, Cai Z. Investigation of ship collision accident risk factors using BP-DEMATEL method based on HFACS-SCA. Reliab Eng Syst Saf 2025;257:110875. https://doi.org/10.1016/j.ress.2025.110875.
[16] Wang H, Chen N, Wu B, Guedes Soares C. Human and organizational factors analysis of collision accidents between merchant ships and fishing vessels based on HFACS-BN model. Reliab Eng Syst Saf 2024;249:110201. https://doi.org/10.1016/j.ress.2024.110201.
[17] Kong D, Lin Z, Li W, He W. Development of an improved Bayesian network method for maritime accident safety assessment based on multiscale scenario analysis theory. Reliab Eng Syst Saf 2024;251:110344. https://doi.org/10.1016/j.ress.2024.110344.
[18] Zhang J, Jin M, Wan C, Dong Z, Wu X. A Bayesian network-based model for risk modeling and scenario deduction of collision accidents of inland intelligent ships. Reliab Eng Syst Saf 2024;243:109816. https://doi.org/10.1016/j.ress.2023.109816.
[19] Govindan K, Chaudhuri A. Interrelationships of risks faced by third party logistics service providers: a DEMATEL based approach. Transp Res E: Logist Transp Rev 2016;90:177–95. https://doi.org/10.1016/j.tre.2015.11.010.
[20] Lee J-S, Yu Y-U. Calculation of categorical route width according to maritime traffic flow data in the Republic of Korea. J Mar Eng Technol 2023;22(5):222–32. https://doi.org/10.1080/20464177.2023.2223396.
[21] Trivedi A, Jakhar SK, Sinha D. Analyzing barriers to inland waterways as a sustainable transportation mode in India: a dematel-ISM based approach. J Clean Prod 2021;295. https://doi.org/10.1016/j.jclepro.2021.126301.
[22] Hong W, Sheng W. A DEMATEL-ISM-BN model of mine water inrush accidents. Mine Water Environ 2023;42(1):178–86. https://doi.org/10.1007/s10230-022-00907-1.
[23] Cao W, Wang X, Zhang W, Li H, Fang S, Yang Z. Data-driven investigation of ship fuel consumption integrating causal inference and hierarchical analysis. Transp Res D: Transp Environ 2026;159:105491. https://doi.org/10.1016/j.trd.2026.105491.
[24] Ugurlu H, Cicek I. Analysis and assessment of ship collision accidents using Fault Tree and multiple correspondence analysis. Ocean Eng 2022;245:17. https://doi.org/10.1016/j.oceaneng.2021.110514.
[25] Yildiz S, Ugurlu O, Wang J, Loughney S. Application of the HFACS-PV approach for identification of human and organizational factors (HOFs) influencing marine accidents. Reliab Eng Syst Saf 2021;208:13. https://doi.org/10.1016/j.ress.2020.107395.
[26] Akyuz E, Arslan O, Turan O. Application of fuzzy logic to fault tree and event tree analysis of the risk for cargo liquefaction on board ship. Appl Ocean Res 2020;101:10. https://doi.org/10.1016/j.apor.2020.102238.
[27] Fiskin R, Cakir E, Sevgili C. Decision tree and logistic regression analysis to explore factors contributing to harbour tugboat accidents. J Navig 2021;74(1):79–104. https://doi.org/10.1017/s0373463320000363.
[28] Gürgen S, Yazir D, Konur O. Fuzzy fault tree analysis for loss of ship steering ability. Ocean Eng 2023;279:10. https://doi.org/10.1016/j.oceaneng.2023.114419.
[29] Qiao WL, Liu Y, Ma XX, Liu Y. Human factors analysis for maritime accidents based on a dynamic fuzzy bayesian network. Risk Anal 2020;40(5):957–80. https://doi.org/10.1111/risa.13444.
[30] Tonoglu F, Atalar F, Baskan IB, Yildiz S, Ugurlu O, Wang J. A new hybrid approach for determining sector-specific risk factors in Turkish straits: fuzzy AHP-PRAT technique. Ocean Eng 2022;253:19. https://doi.org/10.1016/j.oceaneng.2022.111280.
[31] Wang HX, Liu ZJ, Wang XJ, Graham T, Wang J. An analysis of factors affecting the severity of marine accidents. Reliab Eng Syst Saf 2021;210:12. https://doi.org/10.1016/j.ress.2021.107513.
[32] Ozaydin E, Fiskin R, Ugurlu O, Wang J. A hybrid model for marine accident analysis based on bayesian network (BN) and association rule mining (ARM). Ocean Eng 2022;247:16. https://doi.org/10.1016/j.oceaneng.2022.110705.
[33] Fu SS, Zhang Y, Zhang MY, Han B, Wu ZD. An object-oriented Bayesian network model for the quantitative risk assessment of navigational accidents in ice-covered arctic waters. Reliab Eng Syst Saf 2023;238:13. https://doi.org/10.1016/j.ress.2023.109459.
[34] Qiao WL, Guo HTY, Huang EZ, Deng WY, Lian CAP, Chen HQ. Human-related hazardous events assessment for suffocation on ships by integrating bayesian network and complex network. Appl Sci-Basel 2022;12(14):21. https://doi.org/10.3390/app12146905.
[35] Shi J, Liu Z, Feng Y, Wang X, Zhu H, Yang Z, Wang J, Wang H. Evolutionary model and risk analysis of ship collision accidents based on complex networks and DEMATEL. Ocean Eng 2024;305:117965. https://doi.org/10.1016/j.oceaneng.2024.117965.
[36] Bian Y-j, Xie L, Li J-q. Research on influencing factors of artificial intelligence multi-cloud scheduling applied talent training based on DEMATEL-TAISM. J Cloud Comput 2022;11(1):35. https://doi.org/10.1186/s13677-022-00315-4.
[37] Liu H, Yu H, Zhou H, Zhang X. Research on the influencing factors of construction enterprises' digital transformation based on DEMATEL-TAISM. Sustainability 2023;15(12):9251. https://doi.org/10.3390/su15129251.
[38] Ebadi Torkayesh A, Hendiani S, Walther G, Venghaus S. Fueling the future: Overcoming the barriers to market development of renewable fuels in Germany using a novel analytical approach. Eur J Oper Res 2024;316(3):1012–33. https://doi.org/10.1016/j.ejor.2024.02.039.
[39] Li C-W, Tzeng G-H. Identification of a threshold value for the DEMATEL method using the maximum mean de-entropy algorithm to find critical services provided by a semiconductor intellectual property mall. Expert Syst Appl 2009;36(6): 9891–8. https://doi.org/10.1016/j.eswa.2009.01.073.
[40] Singh SP, Sharma A, Adhikari A. Investigating the barriers to drone implementation in sustainable agriculture: A hybrid fuzzy-DEMATEL-MMDE-ISM-based approach. J Environ Manag 2024;371:123299. https://doi.org/10.1016/j.jenvman.2024.123299.
[41] Wang X, Zhang C, Deng J, Su C, Gao Z. Analysis of factors influencing miners' unsafe behaviors in intelligent mines using a novel hybrid MCDM model. Int J Environ Res Public Health 2022;19(12):7368. https://doi.org/10.3390/ijerph19127368.
[42] Uk ZC, Basfirinci C, Mitra A. Weighted interpretive structural modeling for supply chain risk management: an application to logistics service providers in Turkey. Logistics 2022;6(3):57. https://doi.org/10.3390/logistics6030057.
[43] Sternberg A, Carvalho D, Murta L, Soares J, Ogasawara E. An analysis of Brazilian flight delays based on frequent patterns. Transp Res E: Logist Transp Rev 2016;95: 282–98. https://doi.org/10.1016/j.tre.2016.09.013.
[44] Weng JX, Li GR. Exploring shipping accident contributory factors using association rules. J Transp Saf Secur 2019;11(1):36–57. https://doi.org/10.1080/19439962.2017.1341440.
[45] Qin M, Wang X, Du Y. Factors affecting marine ranching risk in China and their hierarchical relationships based on DEMATEL, ISM, and BN. Aquaculture 2022; 549. https://doi.org/10.1016/j.aquaculture.2021.737802.
[46] Ma L, Ma X, Lan H, Liu Y, Deng W. A data-driven method for modeling human factors in maritime accidents by integrating DEMATEL and FCM based on HFACS: a case of ship collisions. Ocean Eng 2022;266:112699. https://doi.org/10.1016/j.oceaneng.2022.112699.
[47] Lin WC. Maritime environment assessment and management using through balanced scorecard by using DEMATEL and ANP technique. Int J Env Res Public Health 2022;19(5). https://doi.org/10.3390/ijerph19052873.
[48] Wang Q, Jia G, Jia Y, Song W. A new approach for risk assessment of failure modes considering risk interaction and propagation effects. Reliab Eng Syst Saf 2021;216: 108044. https://doi.org/10.1016/j.ress.2021.108044.
[49] Cao W, Wang X, Li J, Zhang Z, Cao Y, Feng Y. A novel integrated method for heterogeneity analysis of marine accidents involving different ship types. Ocean Eng 2024;312:119295. https://doi.org/10.1016/j.oceaneng.2024.119295.
[50] Zhang Z, Qin L, Yu JX. Contract & expand: I/O efficient SCCs computing. In: 2014 IEEE 30th International Conference on Data Engineering (ICDE); 2014. p. 208–19. https://doi.org/10.1109/ICDE.2014.6816652.
[51] Arcos-Argudo M, García-López J, Pozo-Coronado LM. Structure of cycles in minimal strong digraphs. Discrete Appl Math 2019;263:35–41. https://doi.org/10.1016/j.dam.2018.06.022.
[52] Lan H, Ma X, Ma L, Qiao W. Pattern investigation of total loss maritime accidents based on association rule mining. Reliab Eng Syst Saf 2023;229:108893. https://doi.org/10.1016/j.ress.2022.108893.
[53] Chen H, Zou Q. Characteristics of wave breaking and blocking by spatially varying opposing currents. J Geophys Res: Oceans 2018;123(5):3761–85. https://doi.org/10.1029/2017JC013440.
[54] Iyer S, Thomson J, Thompson E, Drushka K. Variations in wave slope and momentum flux from wave-current interactions in the tropical trade winds. J Geophys Res: Oceans 2022;127(3). https://doi.org/10.1029/2021JC018003. e2021JC018003.
[55] Xi Y, Hu S, Yang Z, Fu S, Weng J. Analysis of safety climate effect on individual safety consciousness creation and safety behaviour improvement in shipping operations. Marit Policy Manag 2023;50(7):941–56. https://doi.org/10.1080/03088839.2022.2059718.
[56] Lan H, Ma X. Risk evolution analysis of seafarers' unsafe acts in maritime accidents based on directed weighted CN. Appl Sci 2024;14(6):2595. https://doi.org/10.3390/app14062595.
[57] Cao W, Wang X, Shu Y, Li H, Zhou J, Yang Z. An integrated method of advanced optimisation and adaptive ensemble learning for ship fuel consumption prediction. Transp Res C: Emerg Technol 2026;188:105659. https://doi.org/10.1016/j.trc.2026.105659.
[58] Feng Y, Wang H, Xia G, Cao W, Li T, Wang X, Liu Z. A machine learning-based data-driven method for risk analysis of marine accidents. J Mar Eng Technol 2024:1–12. https://doi.org/10.1080/20464177.2024.2368914.
[59] Feng Y, Wang X, Chen Q, Yang Z, Wang J, Li H, Xia G, Liu Z. Prediction of the severity of marine accidents using improved machine learning. Transp Res E: Logist Transp Rev 2024;188:103647. https://doi.org/10.1016/j.tre.2024.103647.
[60] Ma J, Cao L, Feng Y, Karatuğ Ç, Buber M, Wang X. Intelligent analysis of ship collision accidents via low-rank adaptation-based fine-tuning of medium-scale large language models. Reliab Eng Syst Saf 2026;275:112774. https://doi.org/10.1016/j.ress.2026.112774.